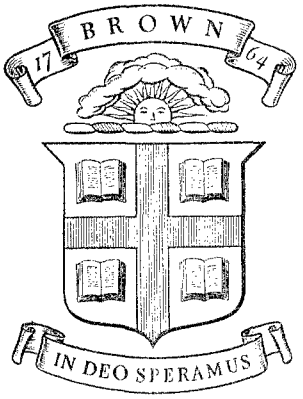

Division of Engineering
BROWN UNIVERSITY
PROVIDENCE, R. I.

BIREFRINGENCE IN ROTATING STRESS FIELDS

C. MYLONAS *and* G. M. BROWN

National Science Foundation
Research Grant G-20259

Department of Defense
Advanced Research Projects Agency
Contract SD-86
Materials Research Program

NSF G-20259/2

ARPA E51

June 1967

BIREFRINGENCE IN ROTATING STRESS FIELDS[1]

by

C. Mylonas[2] and G. M. Brown[3]

Abstract

The transformations of the components of a two-dimensional vibration caused by axis rotation and by a relative phase retardation are used to derive three methods for expressing the changes suffered by polarized light travelling through an inhomogeneous stress field, namely the Poincaré sphere; Neumann's differential equations; and 2x2 complex transformation matrices, and shows their relation with the explicit solution of Drucker and Mindlin. The complex matrix method is applied to the calculation of strain birefringence by alignment and of polarization changes in a stress field with a continuous variation direction and magnitude of principal stress-difference. A comparison with experimental observations shows excellent agreement and indicates some of the difficulties inherent in the problems of birefringence in rotating stress fields. It is hoped that the unified derivation of these methods will facilitate their wider use in photoelasticity.

---

[1] The results presented in this paper were obtained in the course of research sponsored in part by the National Science Foundation under Grant G-20259, by the Advanced Research Projects Agency under Contract SD-86, and by the Division of Engineering, Brown University. This report contains parts of a thesis submitted as partial fulfillment of the requirement for M.S. degree at Brown University.

[2] Professor of Engineering, Brown University, Providence, Rhode Island.

[3] Research Assistant, Brown University, Providence, Rhode Island.

Introduction

The stress-optical relation used in ordinary photoelasticity is strictly valid only in homogeneous stress fields and approximately correct also in fields with stress gradients but without any rotation of the principal directions [1,4]. The laws of birefringence in inhomogeneous stress fields containing azimuth changes of the principal directions are considerably more complicated. Neumann [2] first solved the problem in 1841 for a succession of steps of simple retardation alternating with steps of pure rotation of principal directions (i.e. axis change) and derived the differential equations bearing his name. Drucker and Mindlin [3] have obtained an explicit solution for fields of constant stress difference and constant rate of rotation per unit length. Mindlin and Goodman [4] gave the general differential equations for light propagating in any inhomogeneous state and showed that they simplify into Neumann's equations for harmonic waves and with certain approximations which hardly affect the accuracy for ordinary photoelastic materials and rates of rotation. Their differential equations have not been solved for fields more complicated than the one considered by Drucker and Mindlin. Jones [5,6], Mueller [7], Richartz and Hsu [8] and Aben [9,10] have developed matrix transformations of the components of the light vector passing through birefringent and rotating media. Poincaré [11-14] with a vague reference to M. Mallard introduced an ingenious geometric representation of elliptically polarized light on the surface of a sphere where a simple change of relative retardation corresponds to a rotation about one diameter and a pure axis change by a rotation about a perpendicular diameter. Accordingly Poincaré's sphere is a spherical analog of Neumann's equations. These

results have not been widely noticed and have frequently been re-derived under different forms by other investigators. For example, Menges [15] and Kuske [16] developed a plane geometric representation which corresponds to a modification of a plane projection of Poincaré's sphere. Furthermore the exact similarity between crystal birefringence with rotatory power and stress fields of varying principal direction has not been recognized by all, so that the wealth of information available from physical optics has been frequently ignored in stress-optical studies.

In recent times the effect of the rotation of the principal stresses in photoelasticity has been ignored up to the publication of Drucker and Mindlin's [3] paper. Even then, however, no practical problem with a significant rotational effect was found, so that doubts existed on their importance. More recently rotational effects have appeared to be rather unimportant in some problems [17-19] with strong rotation and significant in others [10, 20-23]. A significant step would be made by learning to distinguish when the rotational effects are important. The most useful result, however, would be to obtain an inverse solution of the stress distribution solely from the total optical effect on light crossing the stress field. At present this problem has not been solved except approximately for a few special cases [10,23] or, for transparent shells, by comparison with the optical effect caused by a large number of stress variations [21,22]. [redacted] General experimental solutions of three-dimensional problems can be obtained when additional information is obtained either by stress-freezing and cutting the model up [24-26], or from transverse observations in scattered light over the whole light path [26,27]. The problem of scattered light in rotating stress fields has been treated by Menges [15] and by Robert [28] who developed special equipment and methods of measurement.

The present paper gives a common derivation and comparison of various apparently different methods of expressing and calculating the birefringence in inhomogeneous stress fields, and uses them in the calculation of birefringence by alignment and of the rotational effects in birefringent coatings. The discussed methods include simple variations of retardation and orientation of the vibration ellipse, the Poincaré sphere, Neumann's equations, Drucker and Mindlin's and Goodman's solutions, 2x2 unitary matrices, and the Stokes vector. It is hoped that this unified derivation will increase their usefulness in photoelasticity and will facilitate the choice of the most suitable method for each problem or the switch from one to another when needed.

Transformation of the Light Vector

The light vector L representing an elliptical vibration at any point of the ray in a transparent medium can be expressed either in coordinate axes u,v parallel to the principal stresses σ_1, σ_2 in the wave-front at that point, or in its own principal ellipse axes $\bar{u},\bar{v}$ (Fig. 1). The direction of propagation $\bar{p}$ is assumed to be outward from the plane of Figure 1 so that the systems σ_1, σ_2, $\bar{p}$ and $\bar{u}$, $\bar{v}$, $\bar{p}$ are right handed. The angle θ is positive when the rotation from σ_1 to OP is right handed (RH) about $\bar{p}$. In axes u,v the elliptic vibration has the form:

$$\left.\begin{aligned} u &= A\cos\theta\cos(\omega t + \varepsilon + \alpha) \\ v &= A\sin\theta\cos(\omega t - \varepsilon + \alpha) \end{aligned}\right\} \quad ; \quad (\theta,\varepsilon) \qquad (1)$$

where $\tan\theta$ is the amplitude ratio, 2ε the relative phase difference, α a common or absolute phase angle and A the intensity

$$\left.\begin{aligned} \tan\theta &= (\max v)/(\max u) \\ 2\varepsilon &= \text{phase } (u) - \text{phase } (v) \\ A &= (\max u)^2 + (\max v)^2 \end{aligned}\right\} \qquad (2)$$

In its own principal ellipse axes $\bar{u},\bar{v}$ at an angle ψ to u,v ($\psi > 0$ when RH from u to $\bar{u}$) the vibration takes the general form:

$$\left.\begin{aligned} \bar{u} &= A\cos\bar{\theta}\cos(\omega t + \bar{\varepsilon}) \\ \bar{v} &= A\sin\bar{\theta}\cos(\omega t - \bar{\varepsilon}) \end{aligned}\right\} \quad ; \quad (\bar{\theta},\psi) \qquad (3)$$

where $\bar{\varepsilon}$ is $\pm\pi/4$ and $\tan\bar{\theta}$ is the amplitude ratio. The exact transformation of (1) into (3) would also require an additional identical phase angle in both components $\bar{u},\bar{v}$. Usually only the relative phase difference of the pair u,v or $\bar{u},\bar{v}$ is needed and the common phase angle is ignored in both.

It is also useful to determine the sense of rotation around the ellipse. This can be recognized from the sign of the only non-zero component of the cross product $\bar{r} \times \dot{\bar{r}}$ of the radius vector and the velocity. The criterion of handedness for $\omega > 0$ is

$$\left.\begin{aligned} &\sin 2\theta\sin 2\varepsilon \\ &\text{or} \\ &\sin 2\bar{\theta}\sin 2\bar{\varepsilon} \end{aligned}\right\} \begin{cases} > 0 & \text{Right-handed (RH) about the direction of propagation} \\ < 0 & \text{Left-handed (LH)} \end{cases} \qquad (4)$$

The vibration at a point is fully determined by the pair of variables (θ,ε) and relations (1) or by the pair $(\bar{\theta},\psi)$ and (3). Transformation of the one pair into the other easily leads to the conditions of equivalence [29]

$$\left.\begin{aligned} \sin 2\theta \sin 2\varepsilon &= \pm \sin 2\bar{\theta} \\ \tan 2\theta \cos 2\varepsilon &= \tan 2\psi \end{aligned}\right\} \qquad (5a,b)$$

$$\left.\begin{aligned} \cos 2\bar{\theta} \cos 2\psi &= \cos 2\theta \\ \cot 2\bar{\theta} \sin 2\psi &= \pm \cot 2\varepsilon \end{aligned}\right\} \qquad (6a,b)$$

The upper of the double signs applies for $\bar{\varepsilon} = \pi/4$, the lower for $\bar{\varepsilon} = -\pi/4$. The transcription relations (5) and (6) will be used here for a simple derivation of the Poincaré sphere, which in turn will lead directly to the complex matrix representation of polarization changes. This common derivation of both representations is much simpler than the usual methods.

Simple Retardation and Pure Rotation

The changes suffered by polarized monochromatic light passing through a homogeneously stressed plate with principal stresses σ_1, σ_2 in the plane of the wavefront are shown in Fig. 2 making a right-handed system with the direction $\bar{p}$ of propagation. The incident plane vibration (0) at an angle θ to σ_1 is decomposed into components u,v parallel to σ_1, σ_2 which travel at different velocities, so that u is accelerated with respect to v by a relative phase difference $2\Delta\eta = 2\pi\Delta N$, where ΔN is the corresponding fringe order in wavelengths. (In some materials the direction of vibration of the faster ray is parallel to the minor principal stress, which could be called σ_1 , but with σ_1, σ_2, $\bar{p}$ right handed). As the phase difference increases from 0 to π the two vibrations compose into the RH ellipses (right-handed about direction of propagation) (1), (2), (3) and for $2\varepsilon = \pi$ into the diagonal (4). As 2ε increases from π to 2π the resultant vibration assumes the shape of the same ellipses as before but described in an LH sense and now

numbered (5), (6), (7), until for $2\varepsilon = 2\pi$ the initial plane vibration (0) is restored. The sequence will be repeated for every increase of 2ε by 2π. If the incident light has the form of any of these ellipses, the sequence should start and return to this ellipse. During these changes of 2ε the magnitudes of max u and max v hence also θ remain constant, but the principal direction ψ_i and the ellipticity $\tan\bar{\theta}_i$ of the ellipse vary. A pure retardation alters only ε and not θ in the representation (θ,ε), but changes both $\bar{\theta}$ and ψ in the representation $(\bar{\theta},\psi)$. On the contrary a pure rotation of axes clearly affects only ψ and not $\bar{\theta}$ in the form $(\bar{\theta},\psi)$, but changes both θ and ε in the form (θ,ε). Accordingly a simple approximate method of calculating the polarization changes would be to simulate the rotating stress field by a series of steps of pure homogeneous retardation $2\Delta\eta_i$ alternating with steps of pure axis rotation $\Delta\phi_i$. The incident vibration is assumed to be written in the local stress axes in terms of (θ_o,ε_o) (1).

a. Increase (θ_o,ε_o) to $(\theta_o,\varepsilon_o + \Delta\eta_1) = (\theta_1',\varepsilon_1')$.

b. Transcribe in new ellipse principal axes, i.e. find (θ_1',ψ_1') with (6).

c. Change axes by $\Delta\phi_1$, i.e. change to $(\bar{\theta}_1,\psi_1' + \Delta\phi_1) = (\bar{\theta}_1,\psi_1)$.

d. Using (5) transcribe in local stress axes in the form (θ_1,ε_1).

Operations a to d are then repeated for each small retardation $2\Delta\eta_i$ followed by a rotation $\Delta\phi_i$, changing $(\bar{\theta},\psi_i)$ into $(\bar{\theta}_{i+1},\psi_{1+1})$. The emerging light vector can be directly transcribed in components parallel with the transmission and extinction axes of a plane polaroid analyzer, the first of which will give the transmitted intensity. Some care is required with the sign of the change $\Delta\psi$: a positive $\Delta\psi$ may be achieved in fixed axes u,v by a <u>right-hand rotation of the ellipse axes $\bar{u},\bar{v}$</u> about the direction of propagation $\bar{p}$, or with a

fixed ellipse but a left-handed rotation of axes u,v about $\bar{p}$. The ellipse rotation may occur by a suitable retardation change (as e.g. from diagonal 4 to ellipses 5, 6 and 7 in Fig. 2) or in a dextro-rotating medium. Accordingly an ellipse rotation is positive when RH; an axis change is positive when LH about $\bar{p}$.

Neumann's Equations

When the changes $\Delta\eta$ and $\Delta\phi$ are small, the resulting changes in ε and ψ can be found by partial differentiation of equations (6) or (7). Assume a light vector at incidence given by (θ,ε) in the stress axes, or by $(\bar{\theta},\psi)$ in its principal ellipse axes at ψ to the stress axes. The pure LH axis rotation $\Delta\psi = \Delta\phi > 0$ leaves $\bar{\theta}$ unchanged but changes 2ε by an amount which is found from the differential of (6b) in $\Delta 2\phi$ for $\bar{\theta}$ constant. After substitution of (6b) and (5a) the differential becomes

$$\frac{\partial 2\varepsilon}{\partial 2\phi}\,\Delta 2\phi = -\cot 2\theta \sin 2\varepsilon\,\Delta 2\phi \qquad (7)$$

The change of 2ε caused by pure birefringence is $\Delta 2\varepsilon = \Delta 2\eta$, which added to (7) will give the total change of 2ε during rotation and retardation

$$\frac{d2\varepsilon}{d2\phi}\,\Delta 2\phi = \Delta 2\eta - \cot 2\theta \sin 2\varepsilon\,\Delta 2\phi$$

Division by $\Delta 2\phi$ and substitution of R for $\Delta\phi/\Delta\eta$ (12), gives equations (7a) below.

The value of θ changes only during rotation but not by retardation, hence is given by the differential of (6a) in ψ for $\bar{\theta}$ = const. After simplification with (6a) and (5b) this gives equation (7b)

$$\left.\begin{aligned} \frac{d2\varepsilon}{d2\phi} &= \frac{1}{R} - \cot 2\theta \sin 2\varepsilon \\ \frac{d2\theta}{d2\phi} &= \cos 2\varepsilon \end{aligned}\right\} \qquad (7a,b)$$

These are Neumann's equations [2,4,30] giving the derivatives of the phase 2ε and amplitude ratio 2θ in the true stress rotation 2ϕ . Ordinary derivative signs are used to show that $d2\varepsilon$ and $d2\theta$ are the total changes from both rotation and retardation. An equivalent pair of differential equations may be obtained for the change of the ellipse orientation ψ and of the ellipticity $\bar{\theta}$ caused by a pure retardation $2\Delta\eta$ and a stress rotation $\Delta\phi$. Equations (5b) and (5a) are now differentiated in $d2\eta = d2\varepsilon$ for $\bar{\theta}$ = constant and $\Delta 2\phi/\Delta 2\eta$ is added to the first to give

$$\left.\begin{aligned} \frac{d2\psi}{d2\eta} &= R \mp \tan 2\bar{\theta} \cos 2\psi \\ \frac{d2\bar{\theta}}{d2\eta} &= \pm \sin 2\psi \end{aligned}\right\} \qquad (8a,b)$$

where the upper of the double signs is valid when $\bar{\varepsilon} = \pi/4$ and the lower when $\bar{\varepsilon} = -\pi/4$. Here $d2\psi$ and $d2\bar{\theta}$ represent the total changes from rotation and retardation and the derivatives are given in terms of the pure birefringence 2η corresponding to the same stresses without rotation. Frequently equations (8a,b) are preferable to Neumann's.

The existence of a light vector $(\bar{\theta},\psi)$ or (θ,ε) remaining invariant with respect to the rotating stress axes along the light ray is found either from equations (8a,b) for $d2\bar{\theta}/d2\eta = 0$ and $d2\psi/d2\eta = 0$, or from (7a,b) for $d2\varepsilon/d2\phi = 0$ and $d2\theta/d2\phi = 0$. Their solution, requiring R = constant , is

$$\left.\begin{aligned} &1)\quad 2\psi_1 = 0,\ 2\bar{\theta}_1 = \pm\tan^{-1}R \\ &2)\quad 2\psi_2 = \pi,\ \bar{\theta}_2 = -\bar{\theta}_1 \end{aligned}\right\} \quad \text{or} \quad \left.\begin{aligned} 2\theta_1 &= \pm\tan^{-1}R, 2\varepsilon_1 = \pm\pi/2 \\ 2\theta_2 &= \pi - 2\theta_1, \varepsilon_2 = \varepsilon_1 \end{aligned}\right\} \qquad (9)$$

where the angle $\tan^{-1}R$ lies in the 1st or 4th quadrants and the upper sign obtains when $\bar{\varepsilon} = +\pi/4$, the lower when $\bar{\varepsilon} = -\pi/4$. The two solutions have identical ellipticity $\tan\bar{\theta}$ but opposite sense, and their major axes are the one parallel, the other perpendicular to σ_1. As will be defined later such vibrations are orthogonal; in fact they fulfill the condition of orthogonality (23).

The Poincaré Sphere

The derivation of the analog representation of the light vector on a unit sphere was given by Poincaré [11-13] as a projection from a complex representation on a plane. It may be simply and directly derived from relations (5) and (6), which have the same form as the transformations between two pairs of spherical coordinates. If a rectangular right-handed system of axes ε, ρ, ψ is chosen (Fig. 3), $2\bar{\theta}, 2\psi$ can be interpreted as latitude and longitude with ψ as pole, the ε-ρ plane as equatorial plane and the circle ψ-ε as prime ψ-meridian. Correspondingly 2θ will be the co-latitude (polar distance) from the ε-pole and 2ε the longitude from a prime ε-meridian coinciding with the ψ-equator. The point P with coordinates $(2\theta,2\varepsilon)$ or $(2\bar{\theta},2\psi)$ will then represent the light vector L in the forms (1) or (3). Any point F on the ψ-equator (or prime ε-meridian) (Fig. 3) represents a plane polarized vibration and its central angle from the ε-pole is twice the angle θ of the vibration with σ_1. In particular the ε-pole represents a plane vibration in the direction σ_1, the ε-antipole a vibration coinciding with σ_2 and point B a plane vibration at 45° to σ_1 and σ_2. The ψ-pole and antipole represent circularly polarized light, respectively right and left handed. A pure

retardation $2\Delta\eta > 0$ will be represented by a right-handed rotation by $2\Delta\eta$ about the ε-axis (Fig. 3), which leaves 2θ unchanged but alters both $2\bar{\theta}$ and 2ψ. Accordingly plane polarized light P passing through a homogeneously stressed plate at an angle θ to σ_1 suffers changes represented by the motion of point P (Fig. 4) on the parallel circle projected along the line PNB. After a retardation 2ε it will be at N, after π at B and after 2π back at P. A pure LH rotation $\Delta\phi > 0$ of the axis system causing an increase in ψ is represented by a right-handed rotation $2\Delta\phi$ of P about the ψ-axis (Fig. 3) which leaves $\bar{\theta}$ unchanged but alters both 2θ and 2ε.

Simultaneous small rotations $2\Delta\eta$ and $2\Delta\psi$, can be added vectorially to give a small rotation $2\Delta\alpha$ about an axis in the ψ-ε plane at an angle 2ρ to the ε-axis (Fig. 5) (positive when RH about the ρ-axis), where

$$2\Delta\alpha = \sqrt{(2\Delta\eta)^2 + (2\Delta\phi)^2} = 2S\Delta\eta \tag{10}$$

and

$$R = \Delta\phi/\Delta\eta \quad , \quad S = \sqrt{1+R^2} \tag{11}$$

$$2\rho = -\tan^{-1}R \quad , -\pi/2 \leq 2\rho \leq \pi/2 \tag{12}$$

Since repeated small increments $\Delta\eta, \Delta\psi$ of constant ratio $R = \Delta\psi/\Delta\eta$ are represented by rotations about the same axis, the process is also valid for simultaneous finite rotations of the same ratio R. A rotation by $2\alpha = 2S\eta$ about an axis in the prime ψ-meridian at an angle $2\rho = -\tan^{-1}R$ to the ε-axis can indeed be shown to correspond to Mindlin and Drucker's solution [3].

The great advantage in using the Poincaré sphere is the direct visualization and easy derivation of properties which otherwise may seem quite complex. For example in the medium of constant rate R of rotation to retardation the poles C and C' of the axis of rotation of the P-sphere (Fig. 5) will not move. Accordingly the elliptically polarized vibrations corresponding to C and C' will be invariant with respect to the local stress axes, i.e. they will rotate unchanged with them, as has already been found from the particular solution of Neumann's equations for R = const. This result is well known in crystal optics: birefringent crystals with rotatory power transmit two such orthogonal elliptically polarized vibrations unchanged, except for rotation.

According to the well known theorem of Euler, the most general rigid body rotation about a fixed point, hence also the most general transformation of incident into emergent light vector, may be achieved by a single rotation about a generic diametral axis (Fig. 6), whether the actual rotation is about the axis, or is made up of partial rotations about any number of other axes giving the same final position of the sphere. This rotation of the sphere as a whole transforms incident light P into N (Fig. 4) or C into C' (Fig. 6), or any other incident light vector D into D' and is a property of the specific birefringent system for a fixed wavelength, not of the parameters of the incident polarized light.

The general rotation is defined either by its axis and angle of rotation or by the initial and final positions C,D and C',D' respectively (Fig. 6) of two points. The rotation of a single point C does not uniquely determine the rotation of the sphere (one may imagine any additional rotation of the sphere about the radius at C'). When C,D are non-diametral

and C',D' are known (respectively two incident and emerging vibrations), the axis of the equivalent single rotation is easily found as the intersection of the planes bisecting and perpendicular to the chords CC' and DD' [11].

As introduced the Poincaré sphere rotations represent the polarization changes of the vibration written in the local (rotated) stress axes. It is frequently required to refer the light vector to fixed space axes. This can be easily done after each step $(2\Delta\phi, 2\Delta\eta)$ by rotating back by $-2\Delta\phi$ from M to M' (Fig. 7). The position of M' in the initial spherical coordinate system gives the light vector in fixed space coordinates. Accordingly the Poincaré sphere can be used also for finding the light vector in space coordinates, by simulating the various steps of pure birefringence as consecutive rotations by $2\Delta\eta_i$ about temporary ε'-axes in the plane of the ψ-equator, each at angle $2\Delta\phi_i$ to the previous one in the same sense about the ψ-axis as the rotation of σ_1 about $\bar{p}$ (LH positive). For example the polarization changes in a medium of constant R will be simulated by consecutive rotations of the sphere by $2\Delta\eta$ about ε'-axes in the plane of the ψ-equator at $2\Delta\phi$ to each other. An elegant equivalent representation, taken from the kinematics of rigid body motion, is the motion of the sphere attached to a circular cone of half angle 2ρ, with ε' (Fig. 5) as axis and the center as apex, tangential to and rolling on the plane of the ψ-equator. All results found with birefringent and rotating systems may be easily derived from this very descriptive representation, used by Poincaré [11] to calculate the rotatory effect of piles of discreet ordered plates (piles of Reusch, treated by Pockels [31], Sohncke [32], and more generally by R. Clark Jones [5]). Poincaré [11] proved essentially that any

polarization change can be produced in a unique way by a simple retarder and a pure rotator plate. Of more immediate interest may be the observation that it may also be achieved by two suitable simple retarders, though this decomposition is not unique. This follows from a more general observation that a rigid body rotation about a center is equivalent with two suitable consecutive rotations about central axes lying in a given plane (here the equatorial plane, Fig. 3).

Stokes Parameters and Mueller Matrices

In 1852 Stokes defined the state of polarization of monochromatic partially polarized light by four quantities, known as the Stokes parameters [29,33]. In terms of the intensities A_1^2 and A_2^2 and the relative phase difference 2ε of the plane polarized components u,v, and of the intensity A_o^2 of the unpolarized component, the Stokes parameters are

$$\left.\begin{aligned} S_o &= A_o^2 + A_1^2 + A_2^2 \\ S_1 &= a_1^2 - a_2^2 \\ S_2 &= 2A_1A_2 \cos 2\varepsilon \\ S_3 &= 2A_1A_2 \sin 2\varepsilon \end{aligned}\right\} \qquad (13)$$

Arranged as a column matrix $\{S_o,S_1,S_2,S_3\}$ they are known as the Stokes vector, very useful for the representation of partially polarized light, whose changes are found by operations with real linear 4x4 operators (Mueller matrices [7]). For completely polarized light of unit intensity the first of (13) gives unity and the other three through the substitutions $A_1 = \cos\theta$, $A_2 = \sin\theta$ as in (1), give the direction cosines (L,M,N) of the radius vector to any point P of the Poincare sphere

$$\left.\begin{aligned} S_1 &= \cos 2\theta = L \\ S_2 &= \sin 2\theta \cos 2\varepsilon = M \\ S_3 &= \sin 2\theta \sin \varepsilon = N \end{aligned}\right\} \qquad (13')$$

and the Mueller matrices degenerate into the 3x3 matrices shown on the right of (16)-(18). Calculations with the Stokes parameters for complete polarization is identical with the process described in page 6 or with rotations of the Poincaré sphere. A much simpler method is obtained when using the two component vector and 2x2 complex matrix operators described in the next paragraph.

Matrix Transformation of Polarized Light

As is usual in optics all transformations of the components (1) of the light vector L are more conveniently carried out in the complex form

$$\left.\begin{aligned} u &= A \cos\theta e^{i(\omega t - \varepsilon + \alpha)} \\ v &= A \sin\theta e^{i(\omega t + \varepsilon + \alpha)} \end{aligned}\right\} \qquad (14)$$

The actual vibration components are given by the real parts of (15) and can be retrieved after any number of linear transformations. In matrix form

$$L = A \begin{bmatrix} \cos\theta e^{-i\varepsilon} \\ \sin\theta e^{i\varepsilon} \end{bmatrix} e^{i(\omega t + \alpha)} \qquad (14')$$

The intensity is $A^2 = L^{+} \cdot L$ ($^{+}$ means conjugate transpose). Frequently only the relative phase difference 2ε is of importance and in addition $A = 1$: then the factor $Ae^{i(\omega t + \alpha)}$ is left out and the unit light vector is written

$$L = \begin{bmatrix} \cos\theta\varepsilon^{-i\varepsilon} \\ \sin\theta e^{i\varepsilon} \end{bmatrix} \tag{14"}$$

As already seen the most general change of polarization at constant energy corresponds to a finite rotation of the Poincaré sphere about a generic central axis, hence the new position of any radius vector could be easily found with the 3x3 transformation matrix of the direction cosines of the new axes in the initial system. However, a much simpler isomorphic representation is obtained with 2x2 unitary matrices. Indeed it can be shown [5,34,35] that the real 3x3 matrix of a rotation of a real 3-component vector in cartesian coordinates has a unique one-to-one correspondence with a 2x2 unitary (complex) matrix operating on a two-component complex vector (u,v) of the form (14).

The most general form of a unitary matrix is [34,35]

$$M = \begin{bmatrix} a & -b^* \\ -b & a^* \end{bmatrix} \tag{15}$$

with

$$aa^* + bb^* = 1 \tag{15'}$$

Asterisks denote the complex congugate. The elements of (15) are known as the Cayley-Klein parameters of the rotation. The operation $M \cdot L$ on the vector L (14) corresponds to a rotation about a general axis. The matrix will be determined first for simple rotations about the coordinate axes. A simple retardation increase by ε corresponds to a RH Poincaré rotation by 2ε about the ε-axis (Fig. 3) and to an operation on $\{u,v\}$ by the retarder matrix $B(\varepsilon)$ (16). Likewise a simple LH rotation ϕ of the axes σ_1, σ_2 (Fig. 1) (or a RH rotation of the polarization ellipse in fixed axes) corresponds to a real RH rotation 2ϕ about the ψ-axis (Figure 3) and to a

transformation of $\{u,v\}$ obtained by operating with the rotator matrix $R(\phi)$ given below (18).

A real right-handed rotation by 2ρ about the ρ-axis (Fig. 3, where 2ρ is shown negative) is achieved by an operation by the matrix $J(\rho)$ (17) on $\{u,v\}$. This rotation does not represent an elementary polarization change but may be used as the equivalent of the consecutive operations $B(-\frac{\pi}{4})R(-\rho)B(\frac{\pi}{4})$ or $R(\pi/4)B(-\rho)R(-\pi/4)$. The complex 2x2 matrix operators for $\{u,v\}$ and their real 3x3 operators for the unit vector (L,M,N) in axes $\varepsilon\rho\psi$ (Fig. 6) are given side by side for comparison.

Simple retarder: Retardation increase 2ε ; P-sphere rotation 2ε

$$B(\varepsilon) = \begin{bmatrix} e^{i\varepsilon} & 0 \\ 0 & e^{-i\varepsilon} \end{bmatrix} \quad ; \quad \begin{bmatrix} 1 & 0 & 0 \\ 0 & \cos 2\varepsilon & -\sin 2\varepsilon \\ 0 & \sin 2\varepsilon & \cos 2\varepsilon \end{bmatrix} \tag{16}$$

Rotation of P-sphere by 2ρ about ρ-axis:

$$J(\rho) = \begin{bmatrix} \cos\rho & i\sin\rho \\ i\sin\rho & \cos\rho \end{bmatrix} \quad ; \quad \begin{bmatrix} \cos 2\rho & 0 & \sin 2\rho \\ 0 & 1 & 0 \\ -\sin 2\rho & 0 & \cos 2\rho \end{bmatrix} \tag{17}$$

Simple rotator: Stress axis rotation ϕ ; P-sphere rotation 2ϕ

$$R(\phi) = \begin{bmatrix} \cos\phi & -\sin\phi \\ \sin\phi & \cos\phi \end{bmatrix} \quad ; \quad \begin{bmatrix} \cos 2\phi & -\sin 2\phi & 0 \\ \sin 2\phi & \cos 2\phi & 0 \\ 0 & 0 & 1 \end{bmatrix} \tag{18}$$

Matrices R , B and J are special forms of the unitary matrix and can be transformed into each other by a suitable axis change.

According to the above the changes of the polarized light passing through a non-absorbing non-depolarizing medium can be found by operating on the complex light vector L (written in the reference axes used to measure azimuths) with a rotator $R(\phi)$ to bring the axes into coincidence with the stress of azimuth ϕ, and on the resulting vector with a retarder $B(\varepsilon)$ effecting a retardation change by 2ε. The resulting vector

$$L_1' = B(\varepsilon_1)R(\phi_1)L_o' \tag{19}$$

will then be given in the rotated axes. An additional operation by $R(-\phi)$ gives the light vector in the initial reference axes

$$L_1 = R(-\phi_1)B(\varepsilon_1)R(\phi_1)L_o \tag{20}$$

Passage through each plate of azimuth ϕ_i and birefringence $2\varepsilon_i$ increases by three the operators in a manner similar to (20). Noting, however, that $R(\phi_{i+1})R(-\phi_i) = R(\phi_{i+1} - \phi_i) = R(\Delta\phi_i)$, the total effect may be put in the form

$$R(\phi_n)B(\varepsilon_n)R(\Delta\phi_{n-1})....R(\Delta\phi_i)B(\varepsilon_i)....R(\Delta\phi_1)B(\varepsilon_1)R(\phi_1)L_o = ML_o \tag{21}$$

The various operators are non-commutative just as finite space rotations but may first be multiplied between themselves in the proper order to give a 2x2 matrix operator M of the general form (15), unitary and with unit determinant as each R and B. This total operator represents the "birefringence" of the non-absorbing non-depolarizing system and may be applied to any incident polarized vector to give the corresponding emerging vector; it corresponds to the total finite rotation of the P-sphere about a general axis and represents the polarization change due to all elements.

The most general form of the operator M (15) may be found in terms of the Euler angles [35] of the corresponding general rotation by 2α [operator $B(\alpha)$] about an axis ε' (Fig. 6) obtained by rotating the initial axis system $\varepsilon\rho\psi$ first by 2ζ about ε [operator $B(\zeta)$] and then by 2ρ about the rotated ρ-axis [operator $J(\rho)$].* Accordingly the general form of M is

$$M = B(\alpha)J(\rho)B(\zeta) = \begin{bmatrix} \cos\rho\, e^{i(\alpha+\zeta)} & i\sin\rho\, e^{i(\alpha-\zeta)} \\ i\sin\rho\, e^{-i(\alpha-\zeta)} & \cos\rho\, e^{-i(\alpha+\zeta)} \end{bmatrix} \qquad (22)$$

The corresponding 3x3 real matrix is more complicated. The general rotation matrix (19) gives the rotated vector in the new coordinate system $\varepsilon'\rho'\psi'$. To write it in the initial system $\varepsilon\rho\psi$, i.e. in the local stress axes, it is necessary to rotate back the axes by -2ρ and -2ζ in this reversed order.

$$M' = B(-\zeta)J(-\rho)B(a)J(\rho)B(a) \qquad (22')$$

Conversely the axis of rotation corresponding to a matrix in the form (15) is found as its eigenvector (two eigenvectors corresponding to diametrically opposite or orthogonal directions) and the rigid body rotation as the matrix of the type $B(\lambda)$ with the two conjugate eigenvalues $\lambda,\bar{\lambda}$ as diagonal elements (interchange of eigenvalues gives the opposite rotation about the opposite axis). The position of the axis and the rotation may also be obtained by writing (15) in the form (22), if necessary by taking out a common factor, and finding ρ, ζ and α.

---

* According to the traditional definition of the Euler angles, the z-axis would coincide with ε, the x-axis with ψ, and the y-axis with $-\rho$.

The intensity of the incident light remains unchanged in non-absorbing media, as has been tacitly assumed when the forms (1) and (15) were introduced (indeed, unitary transformations are energy conserving). Nevertheless, all the present theory may be extended to media with isotropic absorption since the intensity ratio of the components will remain unchanged. The treatment of anisotropically absorbing and birefringent media by complex [2x2] matrices was made by Jones and co-workers [5,6].

General Theorems

The theory of birefringence in rotating stress fields will be completed with some definitions and theorems useful in ordinary applications.

Orthogonal States of Polarization are represented on the P-sphere by diametrically opposite points. Orthogonal plane vibrations P_1, P_2 (on ψ-equator, Fig. 4) are simply perpendicular to each other. More generally vibrations $(\theta_1, \varepsilon_1)$ and $(\theta_2, \varepsilon_2)$ are orthogonal if and only if for k an integer or zero

$$\left.\begin{aligned} 2\varepsilon_2 &= 2\varepsilon_1 + k\pi \\ 2\theta_2 &= \pi + (-1)^k\, 2\theta_1 \end{aligned}\right\} \quad \text{or} \quad \left.\begin{aligned} 2\psi_2 &= 2\psi_1 + \pi \\ \bar{\theta}_2 &= -\bar{\theta}_1 \end{aligned}\right\} \tag{23}$$

Right- and left-handed circularly polarized vibrations (ψ-pole and antipole) are orthogonal, as also are elliptical vibrations of the same axis ratio but with perpendicular major axes and opposite sense.

In complex form orthogonality of two polarized vibration vectors L_1, L_2 is expressed by the relation

$$L_1^{+} \cdot L_2 = 0 \tag{24}$$

The resulting two equations lead directly to (23).

An Elliptic Polarizer or Analyzer admits a specific elliptically polarized vibration of given sense and extinguishes its orthogonal (e.g. the plane polarizer; or the circular polarizer which admits right- but extinguishes left-handed circularly polarized light). Any polarizer is represented on the P-sphere by the point of the vibration it admits; in the complex notation by the corresponding unit vector $\{u,v\}$.

Theorem Every elliptic vibration of unit intensity may be decomposed into any pair of orthogonal vibrations having intensities equal to $\frac{1}{4}$ the square of the chords from their antidiametral points to the point representing the initial vibration.

The theorem is quite easily proved when the initial unit vibration P and the pair of orthogonal components P_1,P_2 are plane, hence are represented by points on the ψ-equator (Fig. 4 and inset).

$$|u_1|^2 = A_1^2 = \cos^2\theta' = \frac{1}{4}(PP_2)^2$$

$$|v_1|^2 = A_2^2 = \sin^2\theta' = \frac{1}{4}(PP_1)^2$$

In general the initial point L and the pair of antidiametral points L_1,L_2 lie on a great circle but can be brought onto the ψ-equator by a single rigid body rotation of the sphere. Such a rotation represents an energy conserving polarization change for each vibration, hence the theorm already proved for the equator is valid in general. To find the intensity, say of L_1 , we call $2e_{o1},2e_{o2}$ the central angles subtended by the arcs (LL_1) and (LL_2) , and note that $e_{o1} + e_{o2} = 90^o$. Then

$$A_1^2 = (\tfrac{1}{2}\text{ chord } LL_2)^2 = \sin^2 e_{o2} = \cos\, e_{o1} = \frac{1}{2}(1 + \cos 2e_{o1})$$

But $\cos 2e_{o1}$ is readily found in handbooks of mathematical geography in terms of the pairs of latitude and longitude $(90-2\theta,\varepsilon)$, $(90-2\theta_1,\varepsilon_1)$ of the end points L,L_1 respectively. Substitution gives

$$A_1^2 = \frac{1}{2}[1 + \cos 2\theta\cos 2\theta + \sin 2\theta\sin 2\theta_1\cos 2(\varepsilon-\varepsilon_1)] \tag{25}$$

In matrix notation the decomposition of a unit vibration L_o into the antidiametral pair is written as

$$L_o = A_1L_1e^{i\alpha} + A_2L_2e^{i\beta} \tag{26}$$

where L_i are unit vectors of the form (14), $L_1^+\cdot L_2 = 0$, A_i^2 are the intensities and α, β phase differences from L_o. Solution for A_1^2 gives again (25).

Corollary: An (elliptic) analyzer receiving elliptically polarized light of unit intensity admits an intensity equal to $\frac{1}{4}$ the square of the chord from the incident point to the analyzer antidiametral point on the P-sphere.

If N is the polarized vibration emerging from a homogeneous specimen (Fig. 4), the intensity admitted through the crossed analyzer A with antidiametral point $A' \equiv P$, will be equal to $\frac{1}{4}(NA')^2$. Clearly as 2ε increases from zero the intensity increases to a maximum of $\frac{1}{4}\sin^2 2\theta$ for $2\varepsilon = \pi$ (point B) and then decreases to zero for $2\varepsilon = 2\pi$ (point P). For parallel polaroids in general no extinction occurs (except when $\theta = 45°$) as the analyzer is at P with antidiametral point at A, and NA is never zero for any point of the parallel circle PNB. This explains why fringe patterns are unclear in a plane polariscope with parallel polaroids, except at points with stress at 45° to the incident vibration.

For a plane analyzer the admitted intensity could be found from eq. (26) with $\varepsilon_1 = 0$, but a more suitable method for computer programming is to rewrite the emerging unit light vector L from local stress axes of azimuth ϕ into principal analyzer axes of admittance azimuth ϕ_A. The admitted intensity will be given by the new u'-component

$$R(\phi_A - \phi)\cdot L = \{u', v'\} \tag{27}$$

It should be remembered that the general polarization change caused by passage through an inhomogeneous anisotropic body corresponds with a single finite rotation of the P-sphere about a generic axis or with an operator of the type (22) applied to the incident polarized monochromatic light of any polarization parameters. Accordingly all that can be achieved by varying the polarization parameters of the incident light and measuring the parameters of the emerging light is the determination of the three Euler angles or parameters in (22). This may be done with two tests employing non-orthogonal incident light vectors. In general, however, the two tests give no information on the actual inhomogeneous stress and birefringence distribution along the light path. This inverse problem of determining the rotating stress distribution from the polarization changes will be discussed in a future paper.

Explicit Solutions

In 1940 Drucker and Mindlin [3] presented an explicit solution of the equations of wave propagation in a medium with constant rate R of stress-axis rotation to retardation. The solution is in a sense approximate because some extremely small terms are neglected. As the only explicit solution, it merits some discussion. The components u,v are given in the local (rotating)

stress axes by means of somewhat intricate expressions in R, S, η (10,11). A simpler form is given here. If light is always written in the standard form (1) in local stress axes, Drucker and Mindlin's solution corresponds to the following expressions for the parameters (θ,ε) of the emerging light in terms of θ_o, ε_o of the incident light

$$\left.\begin{aligned} \tan\theta &= \tan\theta_o \sin\beta_2/\sin\beta_1 \\ \varepsilon &= \beta_1 + \beta_2 - \varepsilon_o \end{aligned}\right\} \qquad (28a,b)$$

where

$$\left.\begin{aligned} \cot\beta_1 &= \frac{S\cos\varepsilon_o - \sin\varepsilon_o \tan S\eta + R\cot\theta_o \tan S\eta}{S\sin\varepsilon_o + \cos\varepsilon_o \tan S\eta} \\ \cot\beta_2 &= \frac{S\cos\varepsilon_o - \sin\varepsilon_o \tan S\eta + R\cot\theta_o \tan S\eta}{S\sin\varepsilon_o + \cos\varepsilon_o \tan S\eta} \end{aligned}\right\} \qquad (29a,b)$$

Accordingly a more general medium of variable R could be approximated by steps of constant R corresponding to consecutive applications of transformation (28). This would be one integration more advanced than taking alternating steps of pure retardation and simple rotation, hence could use larger steps.

Drucker's and Mindlin's results can be easily shown to be a special solution of Neumann's equations (7) for constant R and, though correct, shown an unnecessarily large rotational effect because they give the new components of polarization along the rotated stress axes. A part of the correction is just a transcription of the ellipse of polarization in the new axes and the remainder is the pure rotational effect. Drucker's and Mindlin's correction increases continuously with R and S whereas the

error in the polarization ellipse in fixed coordinates can be shown to be highest for $R = 1$ and to diminish to zero for R tending to zero or infinity.

Drucker's and Mindlin's solution obviously corresponds to the rotation of the Poincaré sphere and the incident light point by $2\alpha = 2S\eta$ about an axis in the ε-ψ meridian at an angle $2\rho = -\tan^{-1}R$ to the ε-axis (Fig. 5). The equivalent operator for such a rotation is given by the matrix M (22) but with $\zeta = 0$. Even then, however, the operation by M would give the light vector in the axis system $\varepsilon'\rho'\psi'$. Premultiplication by $J(-\rho)$ (18) as in (22') should then give the vector in the (local) ε-ψ axes with parameters identical with (29), as may indeed be shown after some lengthy transformations.

Mindlin and Goodman [4] derived the differential equations for light propagation in a general inhomogeneous anisotropic medium. They showed that the general equations transform into Neumann's for harmonic waves, but only after higher order terms are omitted. The neglected terms correspond to the influence of stress gradients across and along the light path as well as to the approximations of Drucker and Mindlin [3]. Accordingly Neumann's equations and all other equivalent representations discussed in this paper are approximate solutions, though of an excellent degree for all practical materials and rates of rotation. No exact explicit solution of Neumann's equations has been obtained for more general distributions than with R = constant. This is no drawback in the determination of the polarization changes in inhomogeneous media, which can be made to any degree of approximation in discreet steps by any of the other methods described. However, the inverse problem of finding stress distributions from polarization changes is greatly hindered.

Applications

1. Strain-Birefringence by Alignment

The high strain-optical sensitivity of certain plastics is produced by partial alignment of random permanently birefringent elements (molecules or crystalline microscopic platelets). The initial randomness insures both macroscopic isotropy and absence of rotatory power: indeed if the elements were orderly distributed, say in cycles of increasing azimuth, they would in general cause a rotation without appreciable retardation [11]. For simplicity assume a very large number N of platelets of constant very small birefringence $0 < 2\eta << \pi$ embedded in a non-photoelastic matrix with their planes perpendicular to the light ray and their principal directions at completely random azimuths ϕ. In the Poincaré sphere the effect of each platelet corresponds to a rotation by 2η about an ε'-axis at 2ϕ to the fixed ε-axis (Fig. 4). Each rotation is extremely small, so that the rotation vectors 2η along the ε'-axes may be added vectorially (Fig. 8), provided the resultant does not become appreciable, say does not exceed the undectectably small relative retardation $2\nu\eta$ of $\nu << N$ parallel platelets. Projection along and across the reference direction gives

$$-2\nu\eta \leq X = \sum_{i=1}^{N} 2\eta\cos 2\phi \leq \nu\cdot 2\eta$$
$$-2\nu\eta \leq Y = \sum_{i=1}^{N} 2\eta\sin 2\phi \leq \nu\cdot 2\eta \qquad (30)$$

which may be considered as the conditions defining randomness provided they hold for any model thickness up to the maximum considered, i.e. for $0 < \nu < N$

the body is then subjected to small strains $\varepsilon_1 \geq \varepsilon_2$ (Fig. 8), respectively along and across the direction of reference without any rotation of these two directions. The maximum engineering shear strain is $2\gamma = \varepsilon_1 - \varepsilon_2 << 1$ and material lines initially of azimuth ϕ are tilted to $\phi - \gamma_\phi$, where $\gamma_\phi = \gamma \sin 2\phi$. Substitution of $\phi - \gamma \sin 2\phi$ for ϕ, expansion and the usual approximation for sine and cosine of small angles give:

$$X \simeq 2\eta \sum_1^N \cos 2\phi_i - 2\eta\gamma \sum_1^N \cos 4\phi_i + 2\eta\gamma N$$
$$Y \simeq 2\eta \sum_1^N \sin 2\phi_i + 2\eta\gamma \sum_1^N \sin 4\phi_i \qquad (31)$$

The first terms in each of (31) are of the order of $2\nu\eta$ or less and the second terms are γ times smaller, hence both are undetectable. Any detectable birefringence will be given by the last term of X, when this term is much larger than $2\nu\eta$, i.e. when $\gamma N >> \nu$

$$X = 2\eta\gamma N \qquad Y = 0 \qquad (32)$$

If all platelets were stacked at alternating azimuths of +45° and -45° (giving no birefringence when unstrained), the same strain would have caused a birefringence $X = 4\eta\gamma N$ or twice as much as for random elements. The method may also be applied to elements with three-dimensional randomness.

Rotational Effects in Birefringent Coatings

The preceding theory and formulas were first checked with a simple trial problem of two plates in plane stress of various intensities and azimuths [43] and were next used in the actual problem of the rotational

effects in birefringent coatings. Birefringent coatings cemented on opaque bodies for the measurement of surface strain by reflected polarized light [36-41] may contain appreciable stress rotations, as e.g. when applied on plates or shells [18,23]. In shells with identical coatings on both faces (Fig. 9) a unique neutral plane exists [18,42] permitting the use of an equivalent cross-sectional area A and moment of inertia I per unit width. On the side $z > 0$ the principal stress differences σ_t and σ_{bz} (at distance z from the neutral plane) caused by principal differences of membrane force $N > 0$ and bending moment $M > 0$ respectively and the corresponding fringe orders n_t and n_b visible in reflected light when each acts alone are

$$\sigma_t = N/A \qquad \sigma_{bz} = Mz/I = \sigma_b z/a \tag{33}$$

$$n_t = 2\sigma_t \Delta h/C_\sigma \qquad n_b = 2\sigma_b \Delta h/C_\sigma \tag{34}$$

where σ_b is the pure bending stress at the coating mid-thickness $z = a$, Δh the coating thickness and C_σ the stress-optical coefficient.

The superposition of membrane and bending stress with principal directions at an angle α (Fig. 10) produces a total principal stress difference σ_z and angle ϕ_z to the major bending plane (plane on which $\sigma_{bz} > 0$ at $z > 0$) which vary with the distance z

$$\sigma_z^2 = \sigma_t^2 [1 + (z\delta/H)^2 + 2(z\delta/H)\cos 2\alpha] \tag{35}$$

$$\cos 2\phi_2 = (\cos 2\alpha + z\delta/H)\sigma_t/\sigma_z \tag{36}$$

where $2H$ is the coated shell thickness and

$$\delta = MAH/NI \tag{37}$$

The rotation and variation of σ_z with z is clearly seen on a Mohr circle construction as in Figure 11. For easier construction all stress states are taken to be pure shears $\sigma_{1t} = -\sigma_{2t} = \frac{1}{2}\sigma_t$, $\sigma_{1b} = -\sigma_{2b} = \frac{1}{2}\sigma_{bz}$, $\sigma_{1z} = -\sigma_{2z} = \frac{1}{2}\sigma_z$, as this leaves their stress difference and birefringence unchanged. The Mohr's circle COD for $\frac{1}{2}\sigma_t$, $-\frac{1}{2}\sigma_t$ is first constructed and the bending stresses $\frac{1}{2}\sigma_{bh}$, $-\frac{1}{2}\sigma_{bh}$ at the interface $z = h$ are added at the points A, B respectively to give the points A_1, B_1 . The length $OA_1 = OB_1$ gives the total principal stresses $\frac{1}{2}\sigma_z$ and $-\frac{1}{2}\sigma_z$ at the interface $z = h$. At the free coating surface $(z = h_1 > h)$ the bending stress $\frac{1}{2}\sigma_{bh1}$, $-\frac{1}{2}\sigma_{bh1}$ is larger, represented by $AA_2 = BB_2$. Now $\frac{1}{2}\sigma_z = OA_2$ at $z = h_2$ and angle $2\phi_2 = DOA_2$. The motion of the segment OA_1 to OA_2 represents the variation of stress magnitude and of double its rotation across the coating thickness. The strongest rate of rotation to stress-difference (retardation) hence the strongest R corresponds to point G , the foot of the normal from O on AA_2 . When G falls between A_1 and A_2 the point of maximum R is within the coating. Obviously the strongest R will develop when G is close to the center O , i.e. when A is close to C and AA_1, AA_2 are respectively shorter and longer than OD , hence when $z > 0$ for $90 < \alpha < 60$ and $\sigma_b \approx \sigma_t$. For $\alpha = 90$, of course, no rotation occurs as σ_t and σ_b are parallel and add algebraically, so that the total stress only changes sign through the value zero without any rotation.

The polarization changes may be easily calculated when the membrane and bending stresses are known. Of greater importance, however, is the inverse problem of using the photoelastic observation to determine membrane and bending stress-differences when both exist and their principal directions are not parallel (otherwise the solution is trivial).

Two approximate solutions of the problem have been given, one [23] for relatively thin coatings but with rotational effects taken under consideration, another [18] for thicker coatings and with the rotational effect partially ignored. The simplicity of the second method and its surprisingly good results make it a reasonable choice for practical applications. It is based on the observation of Drucker and Mindlin [3] that for small values of R the two components of the light vector parallel to the principal stresses at incidence follow the rotating axes without giving rise to strong transverse components. Therefore they should re-emerge from the coating again almost parallel with the surface stresses so that isoclinics corresponding to the surface stress directions should be visible. In addition the relative retardation should be almost proportional with the integrated stress through the coating. (Actually for constant R the retardation at integer fringes is S times larger than without rotation but S is close to 1 for R close to zero). Larger values of R could make the "isoclinics" indistinct and erroneous but, as shown by Fig. 11 and expression (36), large values of R occur over small path lengths in regions of weak stress, which add little to the retardation produced over the remaining path. The stress variation was assumed approximately linear through each coating so that the integrated stress and the visible fringe order could be taken proportional to the stress at the coating mid-thickness. An inverse solution was then obtained for the membrane and bending stress--differences in terms of the fringe orders and the isoclinic parameters observed on the two coatings [18].

The tests had been made with a 9 in. square 0.25 in. thick aluminum plate coated on both sides with 0.107 in. thick layers of specially cast Araldite 6060 resin. The membrane stress consisted of the residual stress

field caused by a central 1 in. diameter shrink-fitted disc. Anticlastic bending was produced by corner loads and was constant within at least the central third of the plate. The values of n_b, n_t and α were known at each point; the total fringe orders and the azimuths of the incident plane polarized light giving a minimum intensity were measured at several points. Tests and calculations were made for a large number of combinations of n_t, n_b and α. The calculated membrane and bending values compared surprisingly well with the true, even under the worst conditions of $n_b \approx n_t \approx 1$ and $60 \leq \alpha \leq 80$ (for $z > 0$), when the isoclinics on each face were very indistinct and doubtful. Furthermore the fringe order seemed to vary slightly with the incident azimuth, as frequently happens with rotating stress. It was decided to calculate exactly the "fringe orders" and the directions of minimum intensity or "isoclinics" and compare them with the observed data.

A computer program based on equations (35,36) was used for the calculation of the relative retardation $2\Delta\varepsilon_j$ due to the average stress in each step without rotation and of the direction change $\Delta\phi_j$ across each step. The step length Δz was automatically adjusted to make the product $|\Delta\phi\Delta\varepsilon| = |R|(\Delta\varepsilon)^2 = (\Delta\phi)^2/|R|$ smaller than 0.03 rad^2, so that large birefringence steps $(\Delta\varepsilon)$ or large rotation steps $(\Delta\phi)$ could be made when R was respectively very small or very large, i.e. when the influence of rotation was small.

The transformation matrix ΔM_i for step i was taken as the average of the matrices found when the rotation step $\Delta\phi_i$ is applied first and the retardation $\Delta\varepsilon_i$ second, and inversely when $\Delta\varepsilon_i$ is first and $\Delta\phi_i$ second:

$$\Delta M_i = \frac{1}{2}\left[B(\Delta\varepsilon_i)R(\Delta\phi_i) + R(\Delta\phi_i)B(\Delta\varepsilon_i)\right] = \begin{bmatrix} \cos\Delta\phi_i e^{i\Delta\varepsilon_i} & \sin\Delta\phi_i \\ -\sin\Delta\phi_i & \cos\Delta\phi_i e^{-i\Delta\varepsilon_i} \end{bmatrix} \quad (38)$$

This matrix approximates the matrix for constant R when both $\Delta\phi_i$ and $\Delta\varepsilon$ are small and tends to the forms $R(\Delta\phi)$ or $B(\Delta\varepsilon)$ (18,16) when $\Delta\varepsilon$ or $\Delta\phi$ tend to zero. The total matrix for the coating was found by multiplying the individual step matrices for inward passage (surface to interface) and then premultiplying this by its transpose, which can be easily shown to be the matrix for reverse passage [5].

The total transformation matrix was calculated for $n_b = 1$ and values of n_t ranging from 0.5 to 2.5 by steps of 0.25. Finally the emerging light intensities were calculated for crossed polarizers with azimuths of the incident light varying from 0° to 90° by steps of 5° and for orthogonal circular polarizers (dark field) with quarter wave plates parallel.

The results for the worst conditions of $60° \leq \alpha \leq 80°$ and $n_b = n_t$ are shown in the graphs of Figures 12-14. Figure 12b shows the fringe and isoclinic pattern close to the shrink-fitted central disc of the plate in anticlastic bending for a bending moment causing by itself one fringe ($n_b = 1$) and the azimuth of the incident plane light at 60° to the major bending direction, which is parallel to the short diameters of the oval fringes. Without any bending the fringes (n_t) are circular, as shown by the thin circles $n_t = 1$, $n_t = 2$ of Figure 12a. The thin dotted lines in Fig. 12a show the contours of equal intensity for the same conditions as Fig. 12b. The area between the contour lines of lowest intensity is shaded and corresponds to the black lines (fringes and isoclinics) of the photograph. The agreement is excellent. The heavy lines (continuous and dotted) of Figure 12a correspond to the calculated fringe pattern in circularly polarized light. As may be seen the change from plane polarized light at 60° azimuth, to circularly polarized light leaves fringes 1 and 1.5 practically unchanged but shifts significantly fringe 2.

The fringe shift during rotation of the crossed polarizers is a characteristic effect frequently noticed in rotating stress fields. It is shown more clearly by the shift of the minima of the curves of Figure 13 representing the intensity observed at points along the 70° radius of Figure 12a (i.e. with an angle $\alpha = 70°$ from principal tension σ_t to principal bending stress σ_b) for incident plane polarized light at azimuths varying from 0° to 75° by 15° (relative to the major bending diagonal). At any one point, however, the intensity still varied with the sine of the angle of the plane of vibration with the principal stress at the surface as may be easily seen in a Poincaré sphere representation.

The experimental values of the angle ϕ_2 of the total stress at the free surface to the major bending plane (Fig. 10) agreed well with the computed values except for $n_b = n_t = 1$ and angles α of 60° and especially 70° and 80°. For $n_b = 1$, $n_t = 2$ the highest divergence appeared again at the same angles α and was much smaller than for $n_t = 1$ except for $\alpha = 80°$. The calculated variation of intensity vs. azimuth of incident light for these cases is plotted in Figures 14a-c. Only the parts of the curves close to their minima are shown. Vertical segments indicate the observed (full segment) and calculated (dotted segment) azimuths of minimum intensity. Horizontal arrows between them indicate a substantial error mainly for $n_t = 1$, $\alpha = 60°$ and to a smaller degree for $n_t = 2$, $\alpha = 80°$. The other errors are much smaller. The probable reason is that the points $n_b = 1$, $n_t = 1$, $\alpha = 60°$ and $n_b = 1$, $n_t = 2$, $\alpha = 80°$ lie on or close to a fringe (the curves for these points rise very slowly from their minima). The isoclinic is then unavoidably determined by the minimum intensity of adjoining areas which get much brighter when the azimuth is varied. But as

shown in Figure 14a, the minima of the points with $n_t = 0.75$ and $n_t = 1.25$ occur at azimuths quite different from those of the point with $n_t = 1$. These azimuths are about -15° for $n_t = 0.75$; 32° for $n_t = 1.00$; and 18° for $n_t = 1.25$. The experimental azimuth of about 2° is in fact the average of -15° and 18°, i.e. the experimenter must have tacitly taken the minimum intensity azimuth midway between those of the bright regions on each side of this fringe. Obviously this procedure, permitted in plane photoelasticity, is invalid in rotating stresses. In all but one instance (Fig. 14b, $\alpha = 70°$ $n_t = 1$), however, the true direction of the surface stress (0 of horizontal scale) was closer to the experimental minimum intensity azimuth (heavy vertical segments) than to the calculated (dotted segments). This provides a justification for the simplifying assumption made in the inverse solution given in reference [18] and an explanation for the obtained accuracy.

Conclusions

A unified derivation of the methods for representing birefringence in inhomogeneous stress fields brings out their direct interrelation. Both representations, by the Poincaré sphere and by the complex vector, afford an easy integration of Neumann's differential equations by three dimensional rotations and by the associated complex 2x2 transformation matrices. Especially simple are the rotations and the relative matrices corresponding to ratios R (twice the rotation to the phase retardation) equal to zero (homogeneous birefringence), or infinity (simple axis rotation), or to a constant. The solution for continuously variable R can be approximated either by consecutive steps with $R = 0$ and $R = \infty$, or better, by steps of constant R . The latter was

found to give an excellent approximation when the product $|\Delta\phi\Delta\varepsilon|$ of rotation by retardation in each step is smaller than $0.03\ \text{rad}^2$.

In the problem of the birefringent coating on a plate subjected to membrane and bending stress, it was found that the azimuth of the incident plane polarized light giving minimum intensity through the crossed analyzer may differ considerably from the azimuth of the principal stress at the surface of the coating, hence that the method of "isoclinics" is invalid. As expected from earlier work [18] the difference is largest when the membrane and bending stress-differences are equal and their principal directions at angles of about 60° to 80° to each other. This error is quite high in regions very close to fringes (retardation close to an integer) where the isoclinic changes with azimuth of incident light in a rapid and irregular way. It appears, however, that the average of the azimuths of minimum intensity on the two sides of a fringe and close to it ($\frac{1}{4}$ fringe away) may be a better approximation of the principal stress azimuth at the fringe center. This permits a significant improvement in the method of photoelasticity in rotating stress fields.

Acknowledgment

The present research was supported in part by the National Science Foundation under Grant NSF G-20259 and in part by the Advanced Research Projects Agency under Contract ARPA SD-86. The authors wish to thank Mr. L. Hermann, research engineer, and Mr. Roger Paul for their help with the tests and photographs and Miss M. Wheat for her care and patience in typing the manuscript.

References

1. Mindlin, R. D., "An Extension of the Photoelastic Method of Stress Measurement to Plates in Transverse Bending," Trans. ASME, Vol. 63, 1941, p. A-187.

2. Neumann, F., "Die Gesetze der Doppelbrechung des Lichtes in komprimierten oder ungleichformig erwärmten unkrystallinischen Körpern," Abh. d. Kon. Akad. d. Wissenschaften zu Berline, Pt. II, 1-254, 1841. Also: Gesammelte Werke, Vol. 3, Leipzig, 1912.

3. Drucker, D. C., and Mindlin, R. D., "Stress-Analysis by Three-Dimensional Photoelastic Methods," J. App. Physics, Vol. 11, No. 11, November 1940, pp. 724-732.

4. Mindlin, R. D., and Goodman, L. E., "The Optical Equations of Three-Dimensional Photoelasticity," J. Appl. Physics, Vol. 20, No. 1, January 1949, pp. 89-95.

5. Jones, R. C., "A New Calculus for the Treatment of Optical Systems, J. Opt. S. A., Parts I, 31 (1941) 488, III 500; IV, 32 (1942) 486; V, 37 (1947) 107; VI 110; VII, 38 (1948) 671; VIII, 46 (1956) 126. Also Hurwitz, H., Jr., and Jones, R. C., Part II, J. Opt. S. A. 31 (1941) 493.

6. Shurcliff, W. A., Polarized Light, Harvard Univ. Press, 1962.

7. Mueller, H., "The Foundations of Optics," J. Opt. Soc. Am. 38, 661 (1948).

8. Richartz, M., and Hsu, H.-Y., "Analysis of Elliptical Polarization," J. Opt. Soc. Am. 39, 136-157, (1949).

9. Aben, H. K., "Photoelastic Phenomena by Uniform Rotation of Principal Axes," Izv. Akad. Nauk. SSSR, Mekh. i Mashinostr. (3), 141-147 (1962).

10. Aben, H. K., "Optical Phenomena in Photoelastic Models by the Rotation of Principal Axes," Exp. Mech. 6 (1), 13-22, 1966.

11. Poincaré, H., "Théorie Mathématique de la Lumière, Paris, Vol. 2, Chapter 12, 1892.

12. Ramachandran, G. N., and Ramaseshan, S., "Crystal Optics," Handbook of Physics, (S. Flugge, Editor), Vol. XXV/1, 1-217, Springer, 1961.

13. Ramachandran, G. N., and Ramaseshan, S., "Magneto-Optic Rotation in Birefringent Media - Application of the Poincare Sphere," J. Opt. Soc. Am. 42, 49-56, 1952.

14. Jerrard, H. G., "Transmission of Light Through Birefringent and Optically Active Media: The Poincare Sphere," J. Opt. Soc. Am. 44, 634-640, 1954.

15. Menges, H. J., "Die Experimentelle Ermittlung Räumlicher Spannungszustände an Durchsichtigen Modellen mit Hilfe des Tyndalleffectes," Z. Ang. Math. Mech. 20 (4), 210-7 (1940).

16. Kuske, A., "Einführung in die Spannungsoptik," Wissenschaftliche Verlaggesellschaft M.B.H., Stuttgart (1959).

17. Mylonas, C., and Drucker, D. C., "Twisting Stresses in Tape," J. Exp. Mech., Vol. 1, 23-32, 1961.

18. Schumann, W., and Mylonas, C., "On the Separation of Membrane and Bending Stresses in Shells with Two Birefringent Coatings," Report DA-4674/5 of the Division of Applied Mathematics, Brown University, July 1960. In final form with the co-operation of R. Bucci, May 1967.

19. Lee, L.H.N., "Effect of Rotation of Principal Stresses on Photoelastic Retardation," Exp. Mech. 4, 10, 306-312 (1964).

20. Wood, A.F.B., "On the Photoelastic Examination of Vibrating Bodies and the Photoelastic Effect in Optically Active Media," J. Mech. Phys. Solids, 8, 26-38 (1960).

21. Kayser, R., "Spannungsoptische Untersuchung von allgemeinen Flächentragwerken unter direkter Beobachtung," Dissertation, T. H. Stuttgart (1964).

22. Kuske, A., "L'analyse des Phénomènes optiques en photoélasticité à trois dimensions par la méthode du cercle de j," Rev. Franc. de Mec. 9, 49-58 (1964).

23. Aben. H., K., "On the Application of Photoelastic Coatings for the Investigation of Shells," Izv. Akad. Nauk SSSR Mekh. i. Mashinostr. 7 (6), 106-111 (1964).

24. Hetenyi, M., "Fundamentals of Three-Dimensional Photoelasticity," J. App. Mech., Trans. ASME, Vol. 5, No. 4, 1938.

25. Frocht, M. M., "Photoelasticity," Vol. II. Wiley, 1948.

26. "Handbook of Experimental Stress Analysis," M. Hetenyi, Editor, Wiley, 1950.

27. Weller, R., "A New Method for Photoelasticity in Three Dimensions," J. App. Phys. 10, 266, 1939.

28. Robert, A., and Guillemet, E., "New Scattered Light Method in Three Dimensional Photoelasticity," Brit. J. Appl. Phys. 15, 567-578, 1964; also, Robert, A. J., "New Methods in Photoelasticity," J. of Exp. Mech., 7, 4, 224-232, 1967.

29. Born, M., and Wolf, E., Principles of Optics, 2nd Ed., MacMillan, 1964.

30. Coker, L.N.G., and Filon, E. G., "A Treatise on Photoelasticity, Camb. Univ. Press, 2nd Ed., 1957.

31. Pockels, F., Lehrbuch der Kristalloptik, Teubner, Leipzig, 1906.

32. Sohncke, L., Math. Ann 9, 504, 1876.

33. Stokes, G. G., Trans. Camb. Phil. Soc. 9 (1852), 399, or his Mathematical and Physical Papers, Vol. III, Camb. Univ. Press, 1901.

34. Jeffreys, H., and Jeffreys, B. S., "Methods of Mathematical Physics," Camb. Univ. Press, 1956.

35. Goldstein, H., "Classical Mechanics," Addison-Wesley, 1965.

36. Mesnager, M., "Sur la Détermination Optique des Tensions Intérieures dans les Solides à Trois Dimensions," Comptes Rendus, Paris, Vol. 190, 1930, p. 1249.

37. Oppel, G., "Das polarisationsoptische Schichtverfaren zur Messung der Oberflächenspannungen am beanspruchten Bauteil ohne Model," Z. VDI, Vol. 81, 1937, p. 638.

38. D'Agostino, J., Drucker, D. C., Liu, C. K., and Mylonas, C., "An Analysis of Plastic Behavior of Metals with Bonded Birefringent Plastics," Proc. of the Society for Experimental Stress Analysis, Vol. XII, No. 2, 1955, pp. 115-122.

39. Fleury, R., and Zandman, F., "Jauge d'Efforts Photoélastique," Comptes Rendus, Paris, Vol. 238, 1954, p. 1559.

40. Zandman, F., "Analyse des Contraintes par Vernis Photoélastique," Groupement pour l'Avancement des Methodes d'Analyse des Contraintes , Vol. 2, No. 6, 1956, pp. 3-14.

41. Duffy, J., "Effects of the Thickness of Birefringent Coatings," J. Exp. Mech., Vol. 1, No. 3, March 1961, pp. 74-82.

42. Gilg, B., "Experimentelle und Theoretische Untersuchungen an dünnen Plätten," Diss. ETH., Ed. Leeman, Zurich, 1952.

43. Brown, G., Master's Thesis, Brown University, June 1967.

CM/mlw

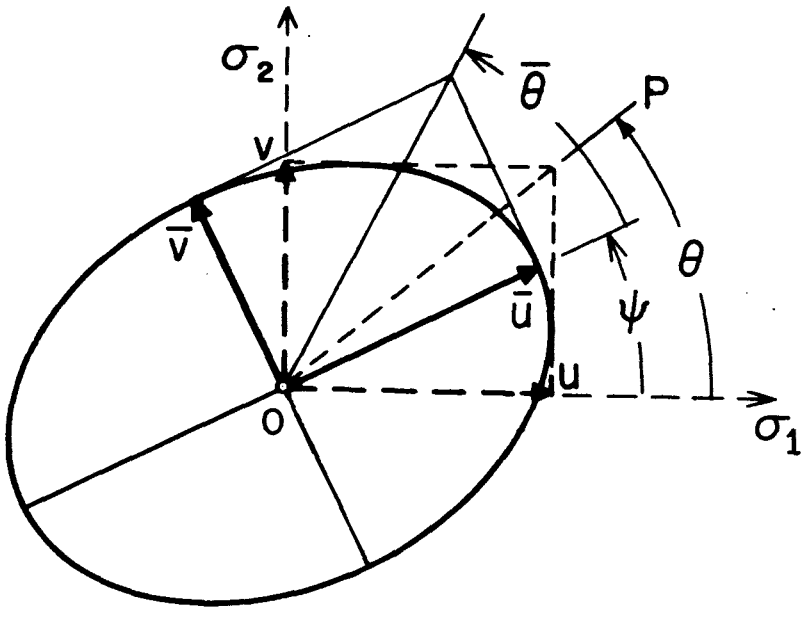

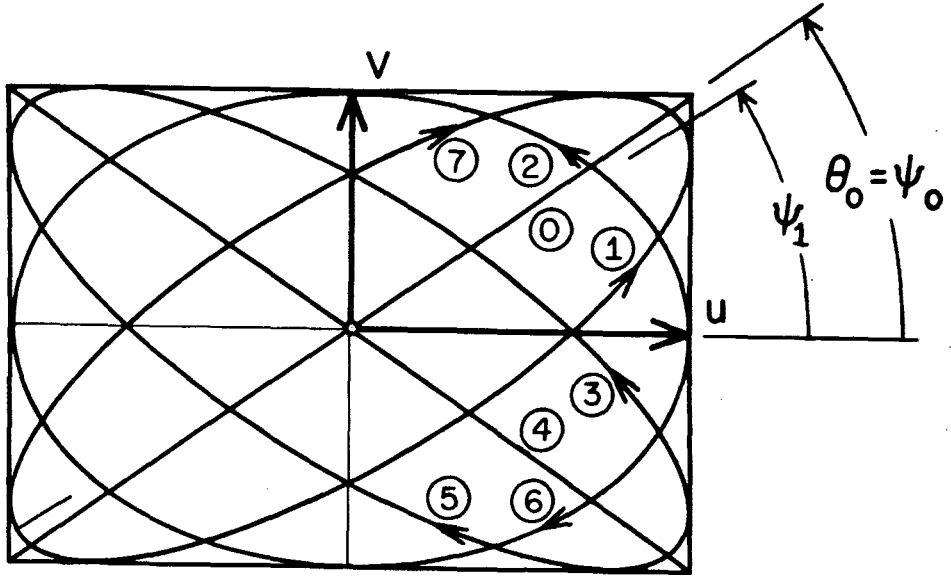

$$\theta,\epsilon \begin{cases} u = \cos\theta\cos(\omega t+\epsilon) \\ v = \sin\theta\cos(\omega t-\epsilon) \end{cases}$$

$$\bar{\theta},\psi \begin{cases} \bar{u} = \cos\bar{\theta}\cos(\omega t+\bar{\epsilon}) \\ \bar{v} = \sin\bar{\theta}\cos(\omega t-\bar{\epsilon}) \end{cases}$$

$$\bar{\epsilon} = \pm\pi/4$$

$$\sin 2\theta \sin 2\epsilon \begin{cases} >0 & \text{RH} \\ <0 & \text{LH} \end{cases}$$

$2\epsilon_0 = 0$ $\qquad$ $2\epsilon_4 = \pm\pi$

$0 < 2\epsilon_1 < \pi/2$ $\qquad$ $2\epsilon_5 = \pi + 2\epsilon_1$

$2\epsilon_2 = \pi/2$ $\qquad$ $2\epsilon_6 = 3\pi/2$ or $-\pi/2$

$\pi/2 < 2\epsilon_3 < \pi$ $\qquad$ $2\epsilon_7 = 2\pi - 2\epsilon_1$ or $-2\epsilon_1$

FIG. 1 ELLIPTICAL VIBRATION IN PRINCIPAL STRESS AXES AND IN PRINCIPAL ELLIPSE AXES.

FIG. 2 VIBRATION CHANGES CAUSED BY PURE RETARDATION

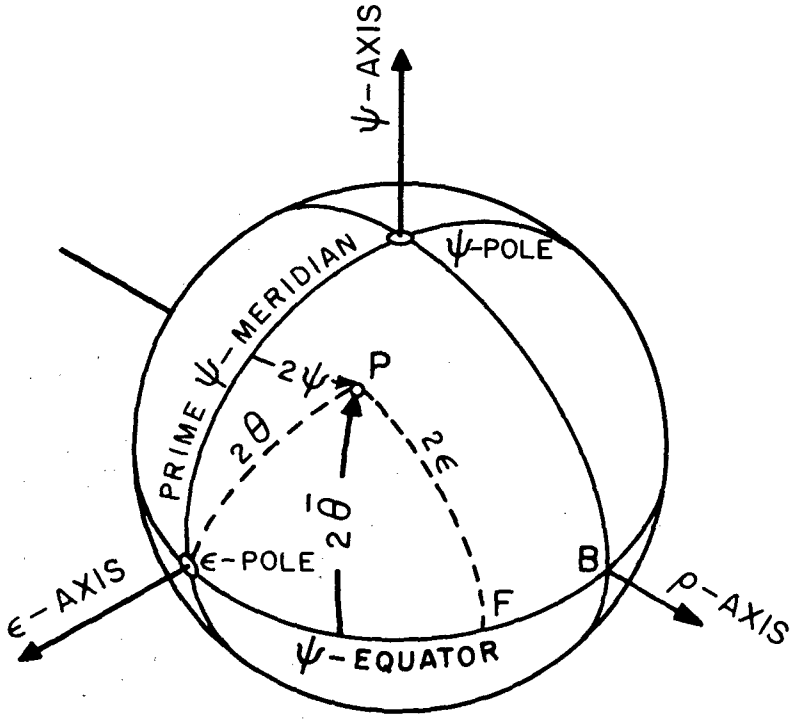

FIG. 3 REPRESENTATIVE POINT $P(\theta, \epsilon)$ OR $P(\bar{\theta}, \psi)$ ON POINCARE SPHERE.

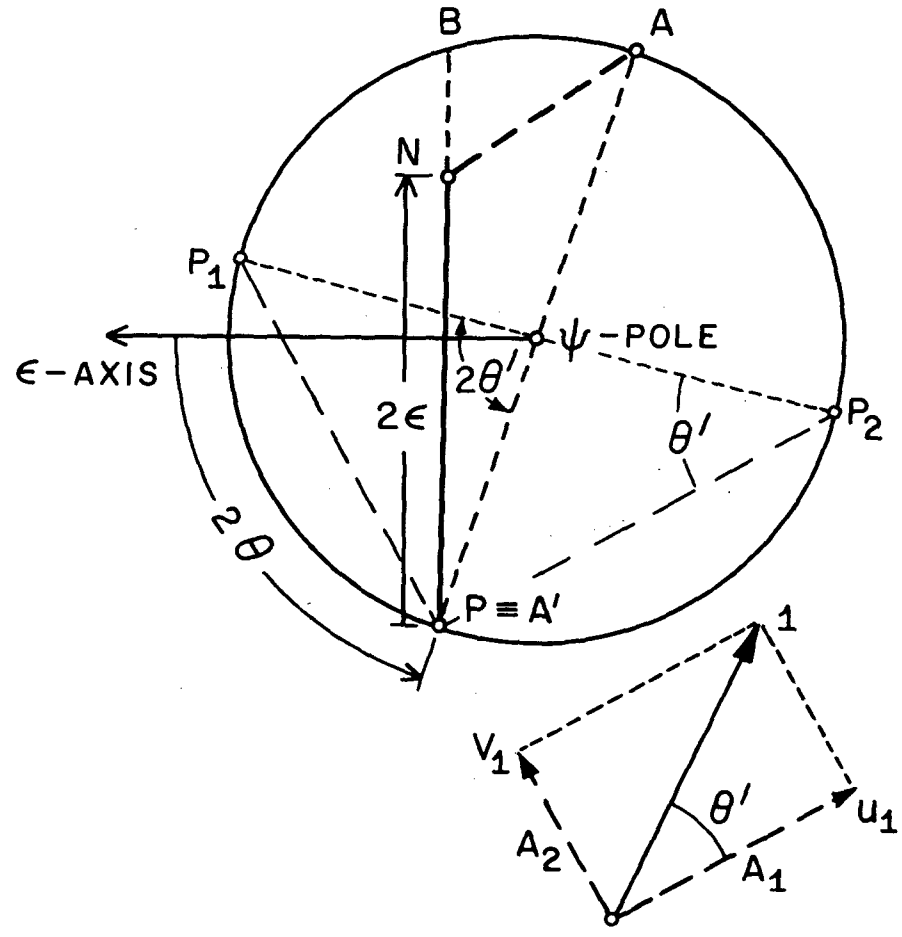

FIG. 4 EQUATORIAL PROJECTION OF PURE RETARDATION CHANGE. INTENSITY ADMITTED BY ANALYZER.

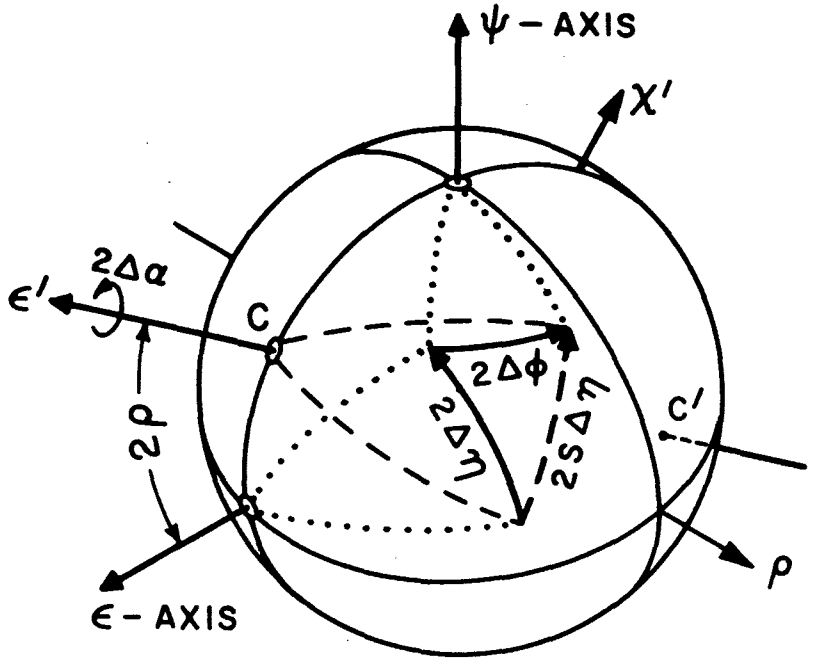

$$2\Delta\alpha = \sqrt{(2\Delta\eta)^2 + (2\Delta\phi)^2} = 2S\Delta\eta$$

$$\tan 2\rho = -R$$

$$R = \Delta\phi / \Delta\eta \qquad S = \sqrt{1+R^2}$$

FIG. 5 SIMULTANEOUS SMALL ROTATION AND RETARDATION.

$$M = \begin{bmatrix} \cos\rho e^{i(\alpha+\zeta)} & i\sin\rho e^{i(\alpha-\zeta)} \\ i\sin\rho e^{-i(\alpha-\zeta)} & \cos\rho e^{-i(\alpha+\zeta)} \end{bmatrix}$$

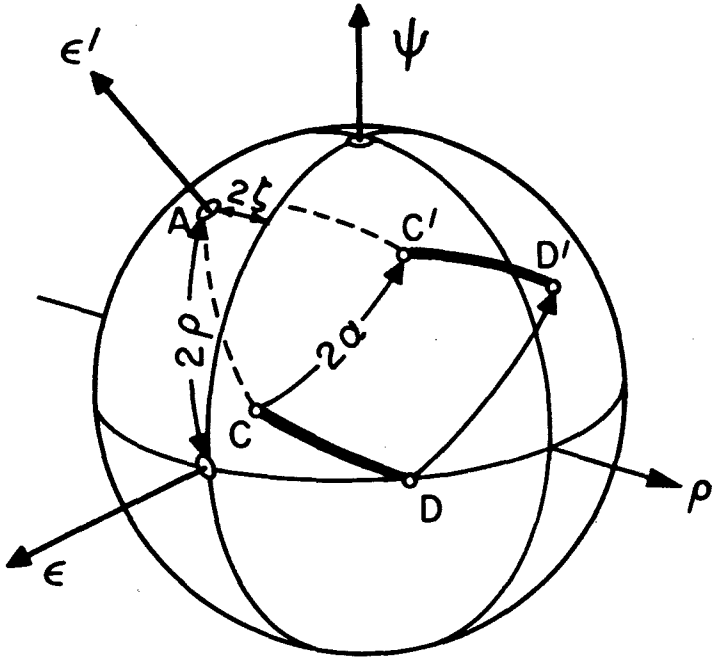

FIG. 6 THE GENERAL POLARIZATION CHANGE

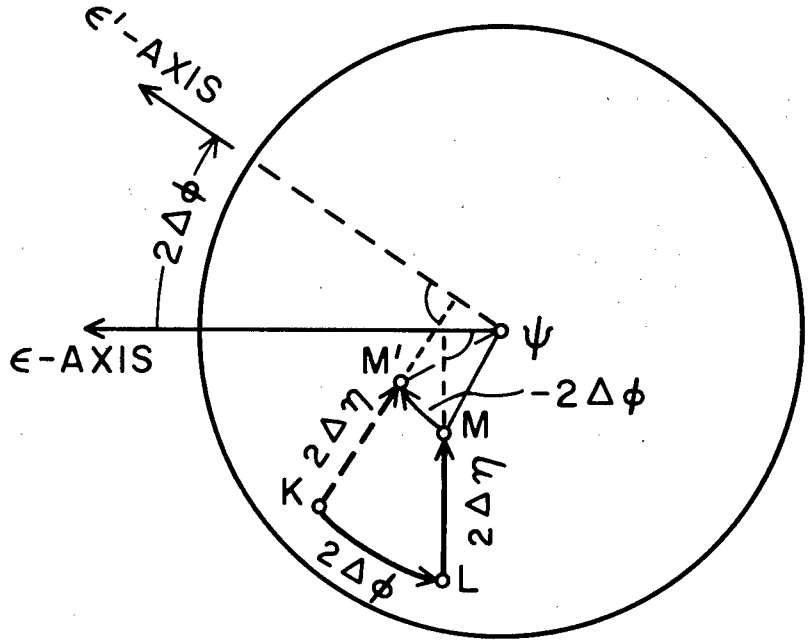

FIG. 7 ROTATION ABOUT ϵ'-AXIS GIVING THE EMERGING VECTOR IN FIXED SPACE COORDINATES.

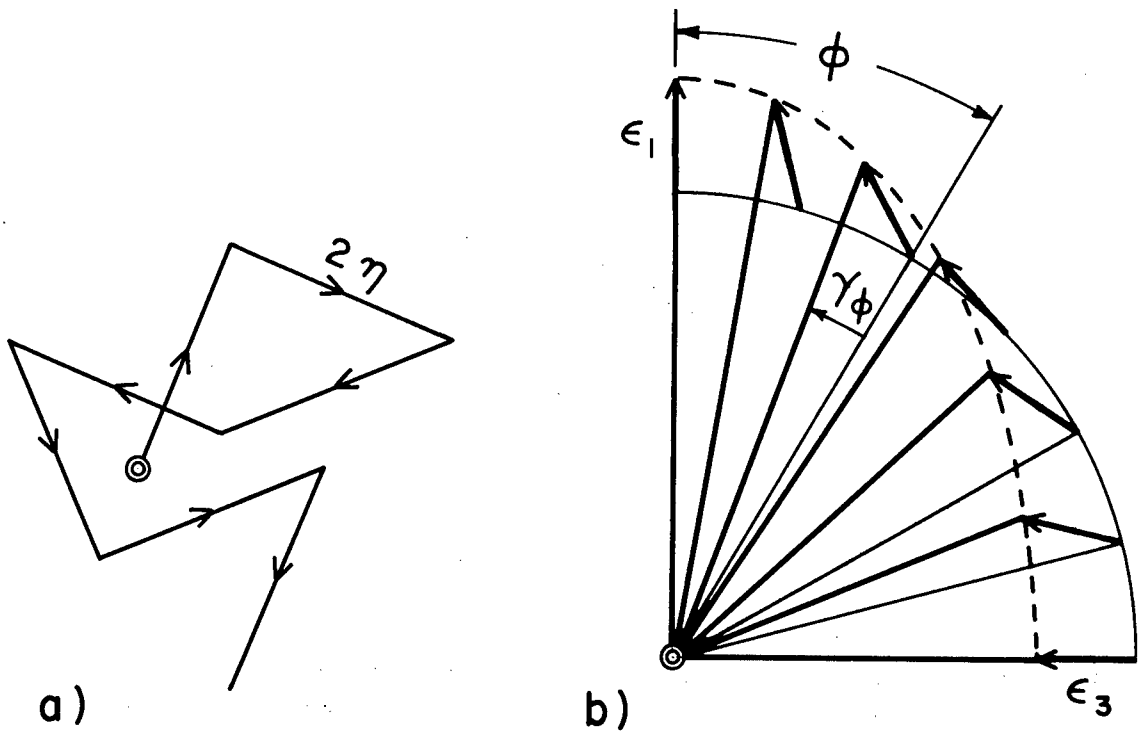

FIG. 8 STRAIN BIREFRINGENCE BY ALIGNMENT OF RANDOM BIREFRINGENT ELEMENTS.

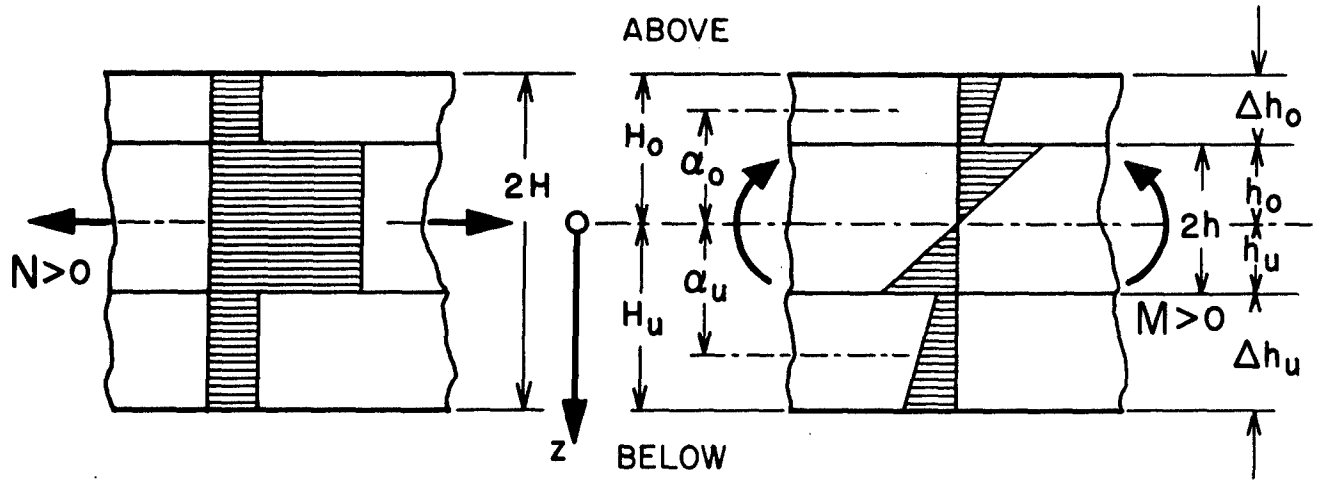

FIG.9 DOUBLY COATED SHELL IN SIMPLE TENSION AND IN PURE BENDING.

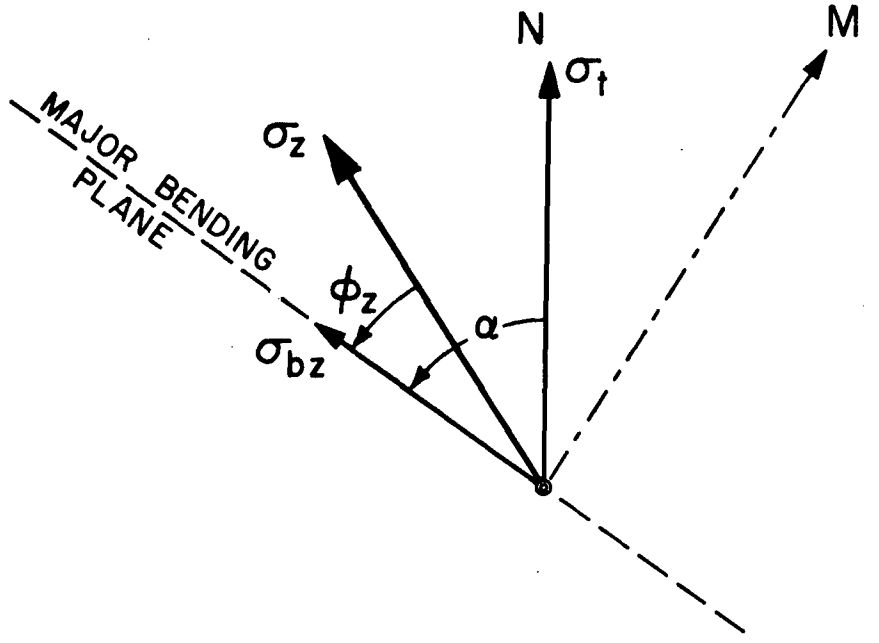

FIG.10 PRINCIPAL DIRECTIONS OF MEMBRANE, BENDING, AND TOTAL STRESS IN THE LOWER COATING, SEEN FROM BELOW (Z > 0).

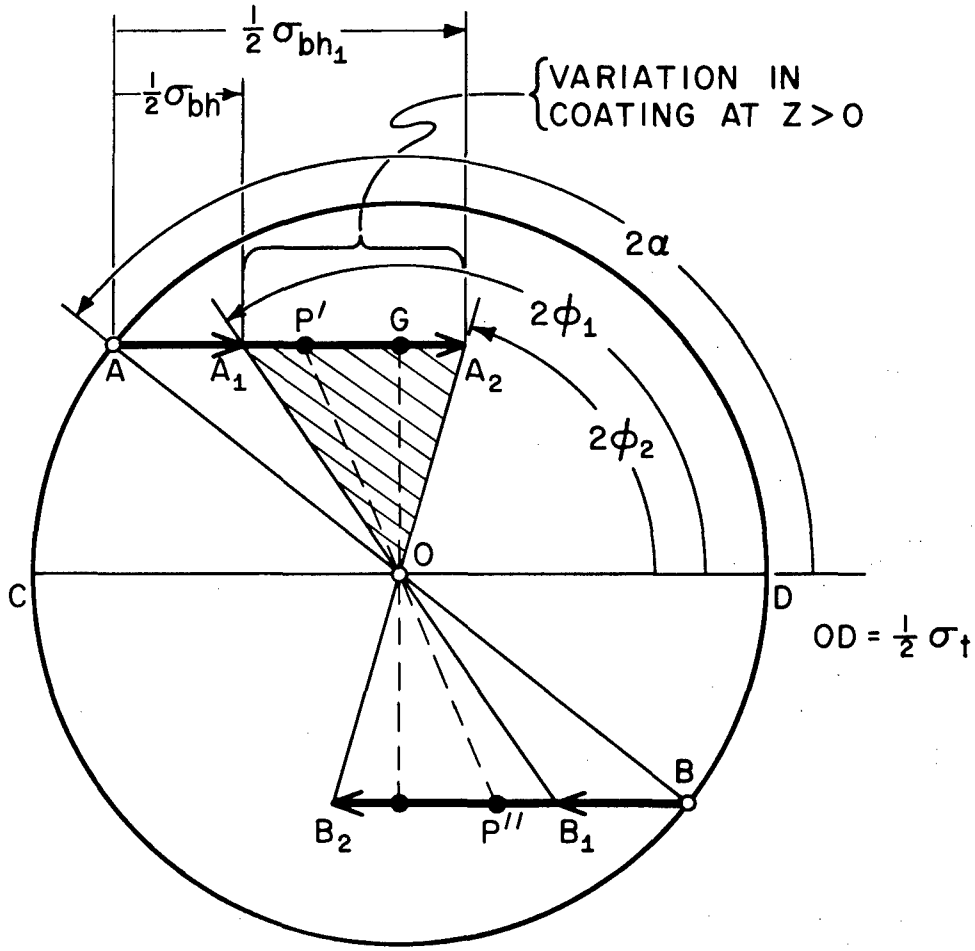

FIG. 11 STRESS VARIATION THROUGH COATING THICKNESS

ROTATION $\phi_2 - \phi_1$ R_{max}

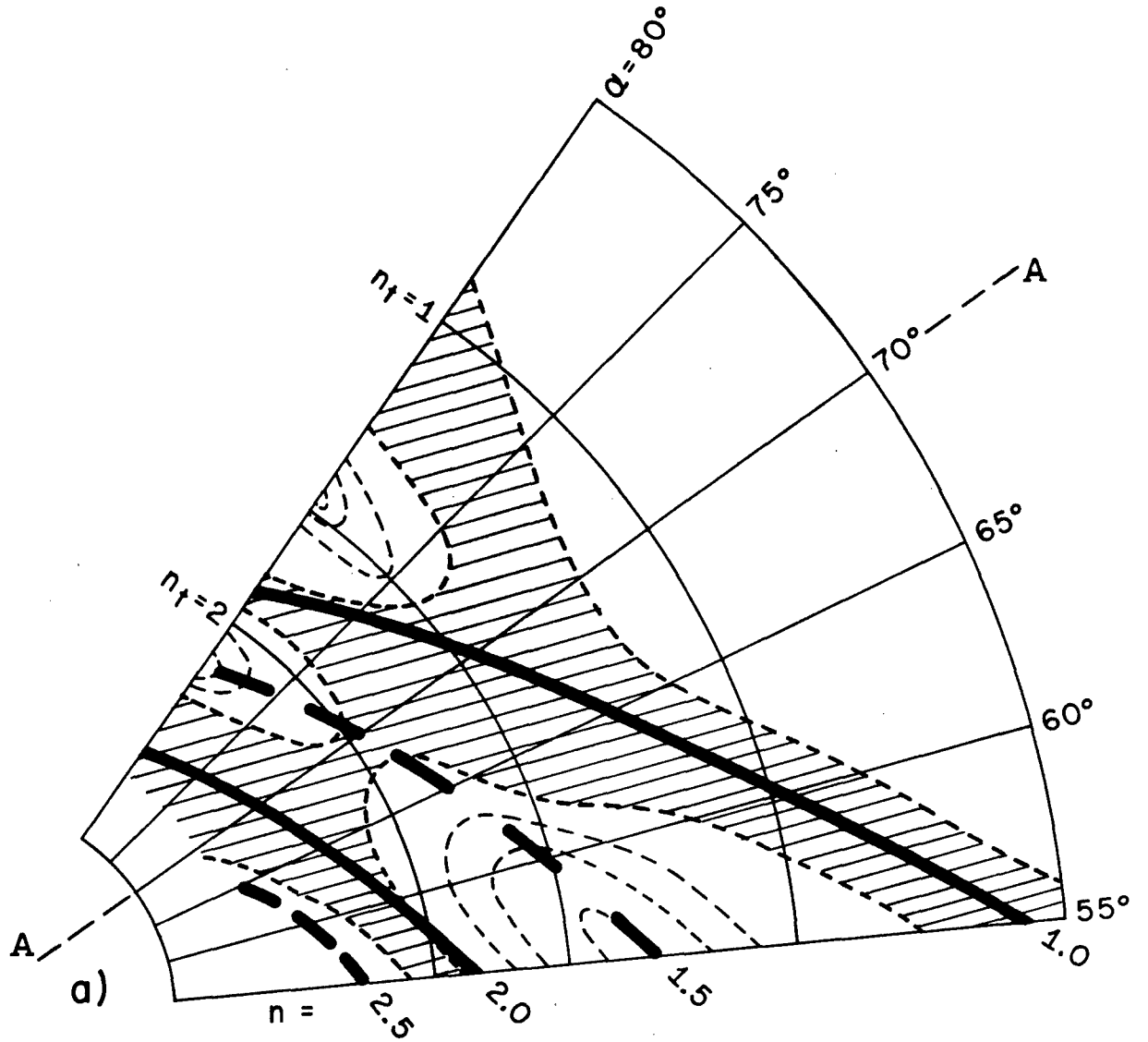

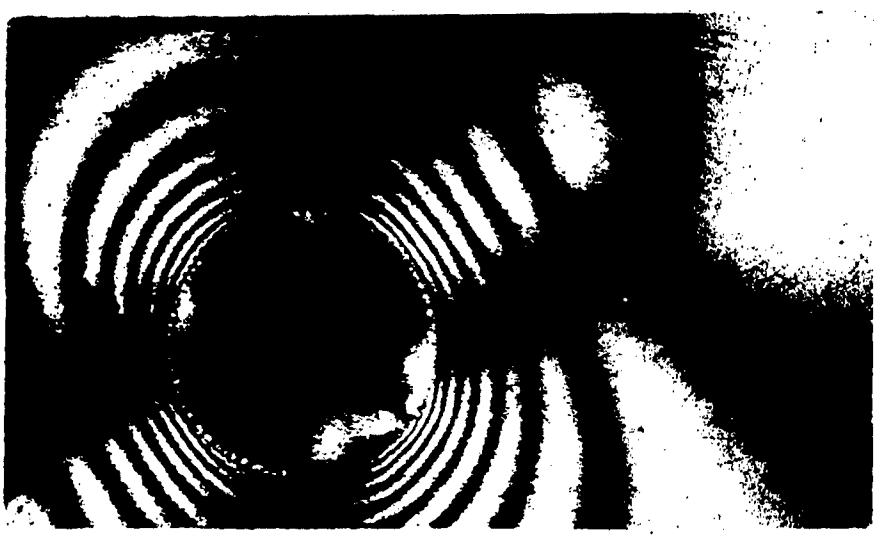

b)

FIG. 12 FRINGE PATTERN AND CALCULATED INTENSITY CONTOURS FOR COATED PLATE WITH SHRINK-FIT STRESSES IN ANTI-CLASTIC BENDING. INCIDENT PLANE-POLARIZED LIGHT AT 60° TO MAJOR BENDING PLANE (PARALLEL TO SHORT AXIS OF OVAL FRINGES

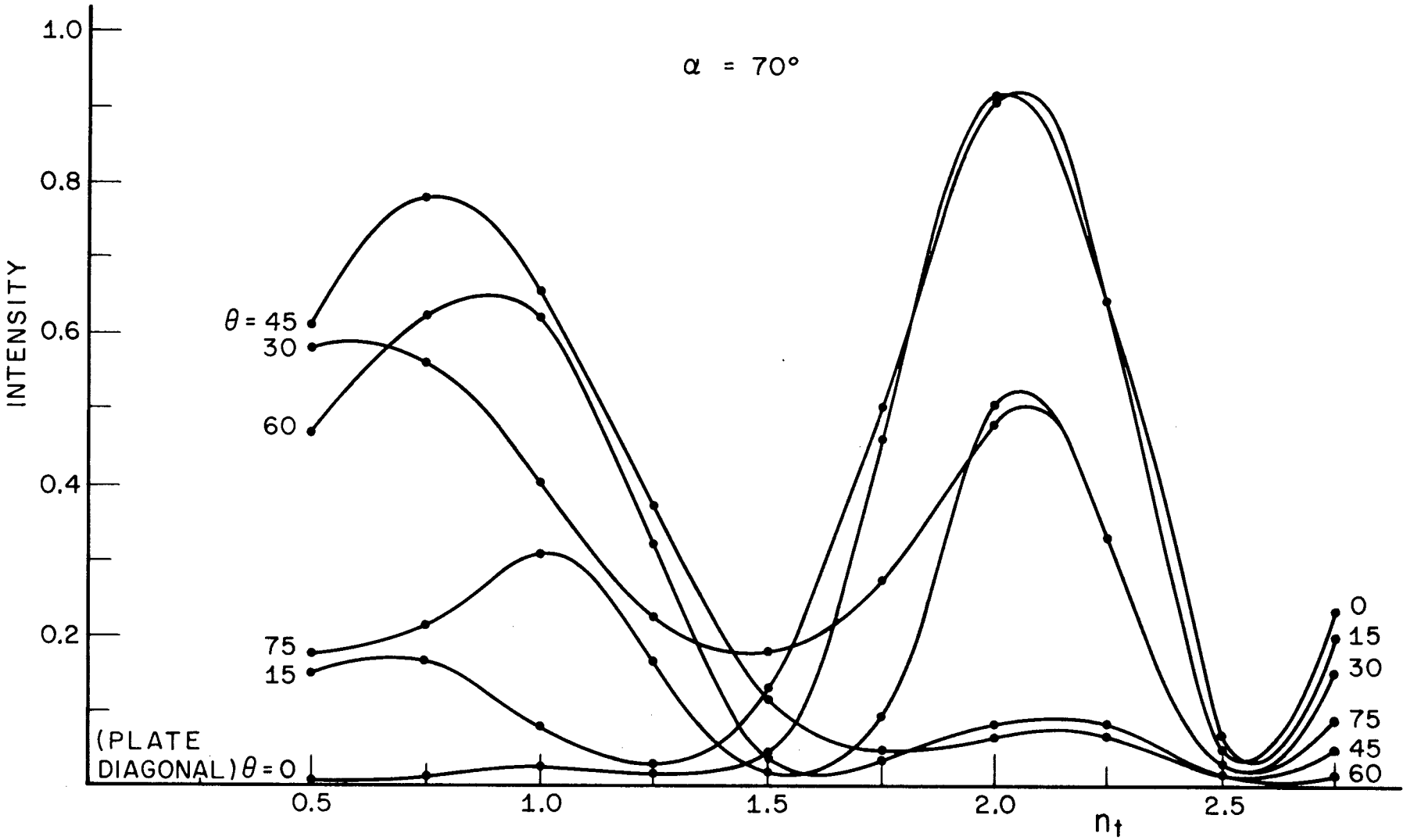

FIG. 13 VARIATION OF INTENSITY ALONG RADIUS 70° ($\alpha = 70°$) FOR $n_b = 1$ AT VARIOUS AZIMUTHS OF INCIDENT PLANE POLARIZED LIGHT.

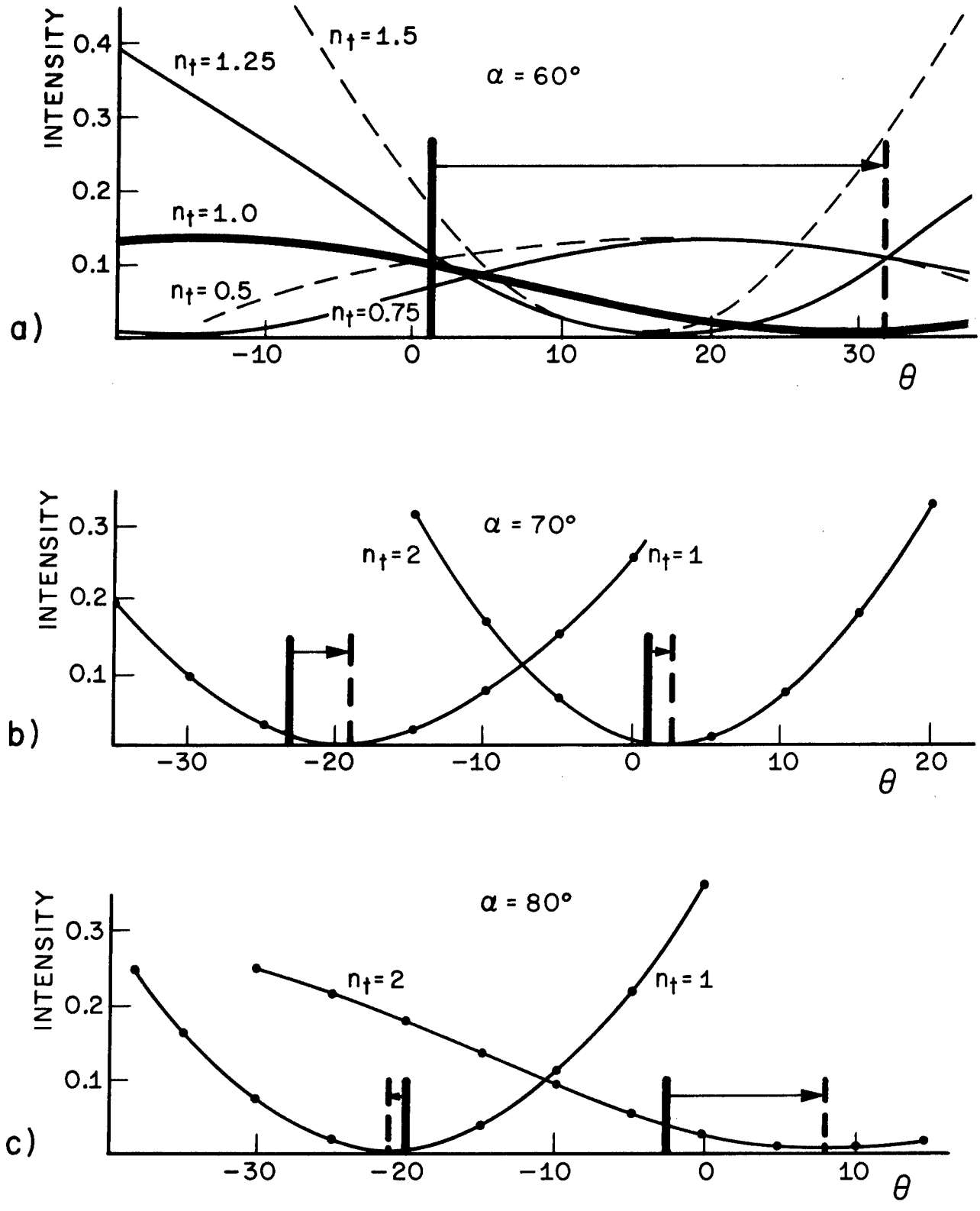

FIG. 14 COMPARISON OF CALCULATED AND OBSERVED AZIMUTHS OF MINIMUM INTENSITY FOR n_t EQUAL TO 1 AND 2 AND α EQUAL TO 60°, 70° AND 80°.